

N74-11806

(NASA-CR-120105) LARGE AMPLITUDE FLUTTER
OF A LOW ASPECT RATIO PANEL AT LOW
SUPERSONIC SPEEDS COMPARISON OF THEORY
AND EXPERIMENT (Princeton Univ.) 85 P
HC \$6.25

Unclas
15846

8% CSCL 01A G3/01

LARGE AMPLITUDE FLUTTER OF A LOW
ASPECT RATIO PANEL AT LOW SUPERSONIC SPEEDS
COMPARISON OF THEORY AND EXPERIMENT

by

C. S. Ventres

C. K. Kang

prepared for
NATIONAL AERONAUTICS AND SPACE ADMINISTRATION
Marshall Space Flight Center

Contract NAS 8-28577

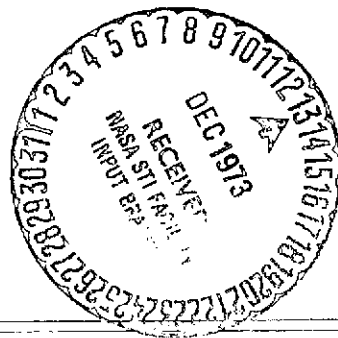
August 1973

PRINCETON UNIVERSITY

Department of Aerospace and Mechanical Sciences
The Aeroelastic and Magnetoelastic Laboratory



AMS Report No. 1116



ABSTRACT

Flutter boundaries, as well as flutter limit cycle amplitudes, frequencies and stresses were computed for a panel of length-width ratio 4.48 exposed to applied in-plane and transverse loads. The Mach number range was 1.1 to 1.4 . The method used involved direct numerical integration of modal equations of motion derived from the nonlinear plate equations of von Karman, coupled with linearized potential flow aerodynamic theory. The results obtained were compared to experimental data reported in Ref. 5.

The flutter boundaries agreed reasonably well with experiment, except when the in-plane loading approached the buckling load. Structural damping had to be introduced, to produce frequencies comparable to the experimental values. Attempts to compute panel deflections or stress at a given point met with limited success. There is some evidence, however, that deflection and stress maxima can be estimated with somewhat greater accuracy.

TABLE OF CONTENTS

	<u>Page</u>
Abstract	i
Table of Contents	ii
Nomenclature	iii
I. Introduction	1
II. Theoretical Development	3
III. Computational Considerations	8
IV. Numerical Results	12
V. Conclusions	20
References	22
List of Figures	23
Appendix	

NOMENCLATURE

a	= panel length
a_n	= modal amplitude
b	= panel width
B_{ijkl}	= nonlinear elastic terms
c	= speed of sound
D	= panel bending stiffness
G_s	= structural damping factor
$g_s \equiv \frac{G_s}{D} \left(\frac{D}{\rho_m h a^4} \right)^{1/2}$	= dimensionless structural damping factor
h	= panel thickness
H_{ji}, I_{ji}	= aerodynamic admittance functions (Eq. 10)
$K = \omega \left[\frac{\rho_m h a^4}{D} \right]^{1/2}$	= dimensionless flutter frequency
M	= Mach Number
N	= number of modes used (Eq. 3)
N_x	= $R_x/R_{x\text{buckle}}$
p	= pressure
$q = \frac{1}{2} \rho U^2$	= dynamic pressure
Q_{ji}	= generalized aerodynamic force (eq. 10)
R_x	= streamwise applied in-plane load
$s \equiv (\lambda^* / \mu)^{1/2} \tau$	= dimensionless aerodynamic time
t	= time

U	= flow velocity
w	= panel deflection
x, y	= coordinates in plane of plate
z	= coordinate normal to plate

Greek

δ_{ij}	= Kronecker delta
Δp	= static pressure differential
$\Delta P \equiv \frac{\Delta p a^4}{Dh}$	= dimensionless static pressure differential
$\lambda^* \equiv \frac{\rho U^2 a^3}{D}$	= dimensionless flow dynamic pressure
$\mu \equiv \rho a / \rho_m h$	= dimensionless flow density
ν	= Poisson's ratio
ρ	= flow density
ρ_m	= panel density
σ_x, σ_y	= panel stresses
$\tau \equiv t \left(\frac{D}{\rho_m h a^4} \right)^{1/2}$	= dimensionless time
ϕ	= velocity potential
Φ	= Airy stress function
ψ_m	= modal function (Eq. 3)
ω	= flutter frequency

I. INTRODUCTION

It is now well established that panel flutter is not, in many cases, an immediately destructive vibration. Hence flutter may be tolerated if it can be established that the flutter amplitude is sufficiently small and the duration of flutter sufficiently short. Unfortunately linear structural and aerodynamic theory is incapable of determining flutter amplitudes. Only by including the important panel nonlinearities can the flutter amplitude be established. Recently, methods have been developed at Princeton for analyzing the large amplitude oscillations of a fluttering plate.¹⁻⁴ In the investigation reported here, these methods were used to calculate the flutter behavior of a panel exposed to a static pressure differential (that is, an applied transverse pressure load), and to applied in-plane compressive loads comparable to the buckling load of the panel.

The panel length-width ratio (4.48), and the range of flow Mach number (1.1 to 1.4) were selected to allow comparison with the results of wind tunnel tests reported in Reference 5. These tests were in turn motivated by a desire to investigate the flutter behavior of certain panels mounted on the forward skirt of the S IV-B stage of the Saturn V launch vehicle.⁵ During these tests, the frequency and amplitude of the panel motion (if any) were measured as the tunnel dynamic pressure was increased. The tests were carried out at various values of test section Mach number, panel static pressure differential, and applied in-plane load. By this method both the panel flutter boundaries (lowest dynamic pressure at which flutter occurred) and the severity of the post flutter motion were determined.

The calculations described herein were carried out for the same range of parameters as used in Ref. 5. The method used involves the direct numerical

integration of a set of nonlinear differential equations for the panel motion, derived from an approximate modal solution of the von Karman nonlinear plate equations. Because of the range of Mach numbers involved, the popular quasi-steady or piston theory expressions for the aerodynamic pressure on the panel were not applicable. Instead the full linearized inviscid, potential flow theory was employed.

So far as is known, the work reported herein constitutes the first attempt at predicting theoretically the severity of flutter of a low aspect ratio stressed panel in the critical low supersonic Mach number range.

II. THEORETICAL DEVELOPMENT

The equations of motion for a three dimensional plate, von Karman's large deflection equations,⁶ are

$$D\nabla^4 w = \frac{\partial^2 \phi}{\partial y^2} \frac{\partial^2 w}{\partial x^2} - 2 \frac{\partial^2 \phi}{\partial x \partial y} \frac{\partial^2 w}{\partial x \partial y} + \frac{\partial^2 \phi}{\partial x^2} \frac{\partial^2 w}{\partial y^2} \quad (1)$$

$$- \rho_m h \frac{\partial^2 w}{\partial t^2} - G_s \nabla^4 \frac{\partial w}{\partial t} - (p - p_\infty) + \Delta p = 0$$

$$\frac{\nabla^4 \phi}{Eh} = \left(\frac{\partial^2 w}{\partial x \partial y} \right)^2 - \frac{\partial^2 w}{\partial x^2} \frac{\partial^2 w}{\partial y^2} \quad (2)$$

where w is the plate deflection and ϕ is the Airy stress function. G_s is a structural damping parameter. The reason for including structural damping will be discussed later. Equation (2) and the first three terms on the right hand side of equation (1) constitute the nonlinear elastic coupling between out-of-plane bending and in-plane stretching that ultimately limits the amplitude of flutter.

Equations (1) and (2) are reduced to a set of simultaneous nonlinear differential equations by Galerkin's method. The transverse displacement w is expressed as a linear combination of modal functions that satisfy the appropriate boundary conditions at the edge of the plate (in this case, those for a clamped plate):

$$w/h = \sum_{m=1}^N a_m(t) \psi_m(x/a) \psi_1(y/b) \quad (3)$$

$$\psi_m(\zeta) \equiv \cos(m-1)\zeta - \cos(m+1)\zeta$$

As is described in greater detail in Refs. 1-4, ϕ is determined by solving equation (2) with expression (3) inserted for w . The boundary conditions satisfied by ϕ on the plate edges (the so-called in-plane boundary conditions) depend on the design of the panel support structure. In Refs. 3 and 4 methods of handling situations corresponding to either complete restraint (no in-plane motion permitted at the edges) or zero restraint (in-plane stresses zero at the edges) are discussed. It is not generally feasible to distinguish between these two alternate sets of boundary conditions beforehand by analyzing the panel support structure (and in fact most practical structures would create a degree of restraint somewhere between the two extremes), so both sets are retained in the developments that follow. With ϕ determined, equation (1) is satisfied in the Galerkin sense by computing the integral average of equation (1) weighted successively by each of the modal functions $\psi_i(x/a) \psi_1(y/b)$ in expression (3) and setting the result to zero. The resulting system of equations is (in nondimensional form):

$$\sum_j S_{ij} (\ddot{a}_j + g_s \dot{a}_j) + \sum_j C_{ij} a_j + \sum_j \sum_k \sum_\ell ijk\ell a_j a_k a_\ell + \lambda^* \sum_j Q_{ji} - \frac{\Delta P}{\sigma} \delta_{1i} = 0 \quad (4)$$

The matrices S and C are the familiar modal mass and elastic stiffness matrices of linear vibration theory. C contains the applied streamwise in-plane tension R_x as a parameter; when R_x decreases below a critical negative value, the plate buckles. The fourth order array B contains the nonlinear terms corresponding to the coupling between in-plane stretching and

and out-of-plane bending referred to previously. Explicit expressions for all of these terms are contained in Ref. 4.

The generalized aerodynamic forces Q_{ji} are defined as

$$Q_{ji} \equiv \int_0^1 \int_0^1 \left(\frac{p_j - p_\infty}{\rho U^2} \right) \psi_i(x/a) \psi_1(y/b) \frac{dx}{a} \frac{dy}{b} \quad (5)$$

where p_j is the pressure on the plate caused by an arbitrary deflection in the j th mode:

$$w \equiv a_j(\tau) \psi_j(x/a) \psi_1(y/b) \quad (6)$$

p_j is given by

$$p_j = -\rho \left(\frac{\partial \phi}{\partial t} + U \frac{\partial \phi}{\partial x} \right) \Big|_{z=0} \quad (7)$$

where the velocity potential ϕ must satisfy

$$\nabla^2 \phi - \frac{1}{c^2} \left(\frac{\partial}{\partial t} + U \frac{\partial}{\partial x} \right)^2 \phi = 0 \quad (8)$$

subject to the boundary conditions

$$\begin{aligned} \frac{\partial \phi}{\partial z} \Big|_{z=0} &= \frac{\partial w}{\partial t} + U \frac{\partial w}{\partial x} && \text{on plate} \\ &= 0 && \text{off plate} \end{aligned} \quad (9)$$

The boundary value problem defined by Eqs. (6-9) has been solved in Ref. 7, where it is shown that

$$\begin{aligned}
 Q_{ji} = & \frac{1}{M} (a_j D_{ji} + \frac{da_j}{ds} S_{ji}) \\
 & + \int_0^s a_j(\sigma) H_{ji}(\sigma) d\sigma \\
 & + \int_0^s \frac{da_j(\sigma)}{d\sigma} I_{ji}(s-\sigma) d\sigma
 \end{aligned} \tag{10}$$

with

$$s = (\lambda^*/\mu)^{1/2} \tau \tag{11}$$

See Ref. 7 or Appendix B of Ref. 4 for evaluations of D_{ji} , S_{ji} , $H_{ji}(s)$, and $I_{ji}(s)$. (Beware of slight notational differences between the two.) These functions depend parametrically on M and a/b , but not explicitly on λ^* and μ . If the integrals in (10) are deleted, the Q_{ji} are those given by "piston theory"; that is by a direct substitution of the well known expression

$$p - p_\infty = \frac{\rho U^2}{M} \left(\frac{\partial w}{\partial x} + \frac{1}{U} \frac{\partial w}{\partial t} \right)$$

into equation (1).

Equations (4) and (10) are combined to form a set of coupled nonlinear ordinary integral-differential equations in time, τ . The solution procedure is to specify λ^* , μ , M , Δp , a/b , R_x , g_s , and to determine the modal amplitudes by numerical integration. Given the $a_n(\tau)$, the deflection

w/h or stresses σ_x , σ_y at any selected point on the panel may be calculated in a straightforward manner. The computer programs used to carry out these various procedures are listed in the Appendix. These routines are modified and improved version of the programs listed in Ref. 4.

III. COMPUTATIONAL CONSIDERATIONS

The considerations of this section relate to the manner in which the computations were arranged and carried out, and to the way in which the results obtained have been displayed. They have been dictated both by the nature of the wind tunnel experiments reported in Ref. 5, and by the necessity of using a very large number of modes (12 in most cases) in order to properly represent the behavior of the low aspect ratio panel being studied.

In order to save computer time (and hence expense) it was found useful to divide the computations into four distinct steps. These are:

1) Computation of the nonlinear terms. Only the plate length width ratio a/b , the Poisson's ratio ν , and the in-plane boundary conditions need be specified in order to determine B . Since the results were to be compared with the data of Ref. 5, only one value of a/b ($= 4.48$) and ν ($= 0.3$) were employed. Hence only two sets of nonlinear terms, corresponding to complete and zero in-plane edge restraint, were required. These were computed at the outset, and stored on magnetic tape.

2) Computation of the aerodynamic admittance functions $H_{ij}(a/b, M, s)$ $H_{ij}(a/b, M, s)$ (see Eq. 10). As indicated, these quantities depend on the panel length-width ratio and the flow Mach number as well as the dimensionless aerodynamic time s . Since only four values of M were studied, it was found worthwhile to compute H_{ij} and I_{ij} beforehand as well (distinct sets of values for each of $M = 1.1, 1.2, 1.3$, and 1.4). They also were stored on magnetic tape.

3) Numerical integration of the panel equations of motion. This operation uses as inputs the data stored from steps 1) and 2) above,

It is therefore convenient to display the results of the flutter amplitude and frequency as functions of q , the (dimensional) dynamic pressure rather than as functions of both λ^* and μ independently:

$$w/h)_p = F(q, M, \Delta p, N_x, g_s)$$

$$K = G(q, M, \Delta p, N_x, g_s)$$

Since the non-dimensionalization of R_x is arbitrary, it has been replaced here by the ratio of R_x to its buckling value:

$$N_x \equiv R_x / R_{x \text{ buckle}}$$

By extrapolating to $w/h)_p \rightarrow 0$, it is possible to determine the critical or flutter dynamic pressure q_f and the flutter frequency K_f :

$$q_f \equiv F_1(M, \Delta p, N_x, g_s)$$

$$K_f = G_1(M, p, N_x, g_s)$$

4) Panel stresses during flutter. In the theory of thin plates, normal stresses vary linearly across the plate thickness. The extreme values of stress occur on the upper and lower surfaces of the panel, e.g.

$$\sigma_x = (\sigma_x)_{ms} \pm (\sigma_x)_b$$

where the $+$ and $-$ sign apply to the upper and lower surfaces, respectively. A similar equation holds for σ_y . The bending stress

$\sigma_x)_b$ is proportional to the local curvature of the plate, and is obtained from the modal amplitudes a_n by differentiating Eq. (3) for w/h . On the other hand, the middle surface or in-plane stress $\sigma_x)_{ms}$ obtained by differentiating the Airy stress function Φ of Eq. (2). As such the in-plane stresses depend not only on the plate deflection $w(x/a, y/b, \tau)$ but also on the in-plane boundary conditions satisfied at the edges of the plate. The computer program listed in the Appendix uses the modal amplitudes $a_n(\tau)$ from step 3) to calculate the in-plane or middle-surface stress for a panel completely restrained at its edges. Since not many flutter calculations were made for the zero edge restraint case, an equivalent program for computing the middle surface stresses in such panels was not written.

IV. NUMERICAL RESULTS

Free Panel Vibrations

In order to explore the extent to which the theoretical model employed mirrors the elastic behavior of the panel, independently of the flutter results, panel natural frequencies were computed as a function of applied static transverse and in-plane loading. The transverse load was equivalent to a pressure differential between the two faces of the panel.

The computations were carried out by integrating the modal equations (4) (with $\lambda^* = \mu = 0$, $g_s > 0$) to determine the equilibrium panel deflection under the assumed loading, and then linearizing the equations about that deflection. The natural frequencies were determined numerically from these linearized equations by solving a classical eigenvalue problem. Representative results are shown in Figures 1 through 4, along with comparable experimental data from Ref. 5.

Figures 1 through 3 show the behavior of modes 1, 2, and 6 under a transverse pressure loading. In each case calculations were made assuming both zero and complete in-plane edge restraint. (The edges of a plate with zero in-plane restraint are free to move in the plane of the plate in response to transverse plate motions, while the edges of a plate with complete in-plane restraint are prevented from making any such movement.) In all three figures there is a systematic discrepancy at zero pressure load. Part of this difference is attributable to imperfect convergence of the solution, but probably not all. The calculated frequencies included in Ref. 5 (Table II) show a similar deviation from the experimental results. Of greater interest, however, are the amounts

by which the various frequencies increase when a pressure load is applied. For the lower modes, the assumption of complete edge restraint provides the best agreement with experiment, while for the higher modes, zero edge restraint works best.

Figure 4 shows calculated and experimental results for the behavior of the ninth mode under a compressive in-plane load. Both calculated frequencies drop off much more near the buckling load than does the experimental curve. This may be due to the presence of imperfections in the plate, such as a slight initial curvature or waviness.

It was not possible, on the basis of these results, to eliminate one in-plane boundary condition from further consideration. Therefore flutter calculations were carried out for both cases, although a shortage of time and money limited the number of zero edge restraint runs that could be carried out.

Flutter Calculations - General Nature of Solutions Obtained

The flutter limit cycle was determined by integrating the modal equations (4) until a periodic motion was found. Experience indicates that the initial conditions used to start the integration do not affect the amplitude or frequency of the limit cycle, at least for $N_x < 1$. Because of the large length-width ratio ($a/b = 4.48$) employed, at least twelve modes were required to obtain an acceptable degree of convergence. Furthermore, the transient portion of the solution survived for the equivalent of many cycles of the ultimate limit cycle motion. (Neither of these statements apply for smaller values of a/b .) As a result, the numerical integration turned out to be costly in terms of both computer memory storage area and computation time.

Initially all calculations were made without introducing any damping other than the aerodynamic damping implicit in the potential flow expression (10) for the generalized forces Q_{ji} . However, it was found that for larger values of the dynamic pressure q the flutter frequency became very high (~ 900 Hz), with the panel deflection being such that the 9th or 10th mode had the largest amplitude. Cunningham⁸ has shown that the flutter frequency and mode shape are both critically sensitive to the amount of structural damping present. Therefore, structural damping was introduced into the panel equations of motion (4) in order to suppress the high frequency flutter.

The structural damping present in the actual panels used in Ref. 5 has not been measured to date. Moreover, if the lower flutter frequency found experimentally is indeed due to the presence of additional damping, the source of that damping need not be structural. It may well be caused by the boundary layer in the airflow over the panel. The capability for dealing with boundary layer effects does exist,⁹ but at least for the present the technique is not practical for flutter calculations involving the use of many structural modes. Hence the introduction of structural damping must be viewed as an essentially ad hoc procedure designed to eliminate a physically unrealistic aspect of the flutter behavior.

From a mathematical standpoint, there are many forms of structural damping that can be introduced into the plate equations to describe non-elastic behavior. Of these the traditional and most popular choice is the $(1 + ig)$ type, which is meaningless for non-sinusoidal motion and is therefore unsuitable for nonlinear plate equations. The most common of the many types that can be used have the general form

$$G_s v^{2n} \frac{\partial w}{\partial t}$$

with $n = 0, 1, 2, \dots$

They differ, in the modal formulation used here, in the relative damping ratios given the various modes. Roughly speaking, the damping ratios increase as the mode number raised to the $(n-1)$ st power. For the present work, $n = 2$ was selected because $G_s v^4 \frac{\partial w}{\partial t}$ fits easily into the modal equations (4), and because it provides greater damping in the higher modes whose motion it is intended to suppress.

Most of the results that follow have been calculated with $g_s = .0001$. This provides a damping ratio for the first mode of .025 (2.5% of critical). Cost limitations have made it impossible to present a systematic study of the influence of structural damping over the complete range of Mach number, static pressure differential, and applied in-plane load considered here.

Flutter Boundaries

Figures 5 and 6 show flutter boundaries as a function of Mach number for an unloaded panel ($\Delta p = N_x = 0$). Curves are shown for $g_s = 0$ and $g_s = .0001$. On the same figures are shown experimental data from Ref. 5. The data were obtained from several different panels (of identical specification), and for two different boundary layer thicknesses, the thicker one being induced by inserting spring pins in the tunnel wall ahead of the panel, which was mounted flush to the wall. This caused the boundary layer thickness (as measured near the trailing edge of the panel) to increase roughly 7 to 30%, depending on the tunnel Mach number and dynamic pressure.⁵

Both the theoretical and experimental results show a gradual decrease in flutter dynamic pressure with increasing Mach number, but the theory shows no minimum at $M = 1.3$. The theoretical flutter boundary for $g_s = 0$ agrees best with the experimental results for the smooth wall boundary layer (Figure 5) while the damped flutter boundary agrees best with the results for the rough wall boundary layer (Figure 6). This is the correct qualitative behavior, since the boundary layer introduces a damping effect that increases with boundary layer thickness. The quantitative agreement in Figure 6 is of course fortuitous, since the amount of structural damping introduced is arbitrary, and in any event the damping is of structural origin in the theory and aerodynamic in the experiment.

Flutter frequencies are shown in Fig. 7. As mentioned previously, the frequencies for zero damping are unrealistically high, whereas those for $g_s = .0001$ are comparable to the experimental results. Neither theory nor experiment shows much variation with Mach number.

Figures 8 and 9 show calculated and experimental flutter boundaries for plates exposed to compressive in-plane loads. In both figures the qualitative behavior with N_x is correct, although the rate of decrease in the flutter dynamic pressure is more rapid according to the theory. Near buckling ($N_x = 1.0$), the theoretical result becomes overly conservative. The calculations of flutter boundaries near the buckling load is a difficult matter, since the plate behavior is then especially sensitive to the presence of small initial structural imperfections, to the damping effect of the boundary layer, and so on. The prediction of panel natural frequencies under in-plane loading suffers the same difficulty, as can be recalled from Fig. 4.

Figure 10 shows a limited set of calculations for a panel exposed to a static pressure differential. Both sets of in-plane boundary conditions (zero and complete edge restraint) are included. The line labeled "Exp." is a derived curve taken from Fig. 43 of Ref. 5. The result for zero in-plane restraint shows the better agreement with experiment, in spite of the fact that the panels referred to in Ref. 5 were carefully mounted in a massive supporting structure. This result is consistent with similar comparisons made previously involving panels of smaller length-width ratio at higher Mach numbers.^{3,10}

Figs. 11, 12, and 13 contain flutter boundaries for panels exposed to combined loading (both $\Delta p \neq 0$. and $N_x \neq 0$.). The theoretical results are all for the case of complete edge restraint, and reflect the same behavior as exhibited in Fig. 10, namely, a lack of sensitivity to static pressure differential. Note, however, that the agreement between the slopes of corresponding pairs of flutter boundaries in Fig. 11 improves as the in-plane loading increases.

It would be desirable to carry out calculations equivalent to those shown in Figs. 11-13 for the zero in-plane restraint case.

Panel Displacement in Flutter

A record of panel centerline deflection during approximately one period of the flutter oscillation is shown in Fig. 14. Structural damping ($g_s = .0001$) was assumed in making the calculation; with no damping, many more zero crossings appear than are shown. The motion portrayed in Fig. 14 is qualitatively similar to that reported in Ref. 5. (See especially Fig. 57 of that report). In particular, the panel deflection is largest near the trailing edge, but not markedly so, and the streamwise variation of the

deflection is elaborate, but with relatively few zero crossings at any given instant. The motion has a quasi wave-like character, since the zero crossings (points of zero deflection) move with time, and even appear and disappear.

Relatively little panel displacement data was published in Ref. 5, and what was presented was limited to a case wherein the panel was buckled by the applied in-plane load. This situation is both the most important physically (since at a given dynamic pressure the panel deflection is maximized), and the most difficult to handle analytically. As mentioned previously, buckled panels are especially sensitive to effects that normally are either ignored entirely (such as initial imperfections), or handled very crudely (structural damping).

Panel displacements at three different streamwise locations (but 2.5 inches off the centerline) are shown in Fig. 15. The streamwise locations of probes A, C, and F are shown in Fig. 14. At all three locations, the calculated displacements are considerably larger than their experimental counterparts.

Stresses

The bending stresses are generally considerably larger than the in-plane or axial stresses during flutter. Since the bending stresses are proportional to local panel curvature, the bending stress distribution generally resembles the panel deflection (see Fig. 16). Attempts to compute stresses at a given point on the panel are therefore hampered by the same difficulty encountered in calculating deflections: a small change in the flutter mode shape causes large errors in the stresses computed at that point.

Fig. 17 shows a comparison of calculated and experimental stresses as a function of flow dynamic pressure for a buckled panel. The open circles are the peak-to-peak bending stress in panel #6 at the location of gauge B1, just off the center line of the panel near its trailing edge. The small triangles connected by straight lines are theoretical peak-to-peak stresses calculated for the same point, as well as for a point on the panel center-line, three quarters of the way back behind the leading edge. This latter location is the point where the maximum stress occurred, according to the theory. It should be noted that the applied in-plane load assumed for the calculations was only 73.5% of the theoretical buckling load, whereas the experiment was carried out with an in-plane load equal to 96% of the buckling load applied. As can be seen, the bending stress computed at the 3/4 chord point agrees better with the experimental result than does the value computed at the position of gauge B1. If the stress measured at B1 is in fact the maximum stress that occurred, then the maximum stress is computed with greater accuracy than is the stress at B1.

Figs. 18 through 21 (each of which is divided into two parts) show similar comparisons. In each figure part (a) shows theoretical and experimental bending stresses (Figs. 18 and 19) or axial stresses (Figs. 20 and 21) at the point referred to above. In part (b) the calculated data is the theoretical maximum stress on the panel, displayed alongside the same experimental data as in part (a). In general, the maximum stress (which is less sensitive to changes in the flutter mode shape) best reflects the experimental trends, at least for small N_x . Near the buckling load, excessively large maximum stresses are predicted, presumably for the same reasons mentioned earlier.

V. CONCLUSIONS

Flutter boundaries were computed numerically as functions of Mach number, in-plane loading, and static pressure differential. Comparison with experimental data indicate reasonably good correlation for Mach number and in-plane loading, except near the buckling load. The influence of static pressure differential depends on the in-plane boundary conditions assumed. Assuming zero restraint (edges free to move in plane) provided the best correlation with experiment, although not enough calculations were made to firmly establish this point.

The flutter mode shapes calculated were in good qualitative agreement with experiment. The flutter frequency, however, proved to be sensitive to the amount of structural damping assumed. With no damping, the coupled flutter frequency was several times higher than the experimental value. Because flutter frequency is an important factor in determining panel fatigue life, future experimental programs should include a determination of panel damping. In addition, the theoretical model employed should be improved to include the damping effect of the boundary layer.

Attempts to compute panel deflection and stresses during flutter met with limited success, particularly for buckled panels. There is some indication, however, that maximum deflections and stresses can be calculated with greater accuracy than deflections or stresses at a specific point. From a practical standpoint, knowledge of the maximum is sufficient to determine panel fatigue life; the stress distribution and mode shape are of lesser significance.

Most of the difficulties encountered in this investigation stem from the large length-width ratio of the panel and the presence of

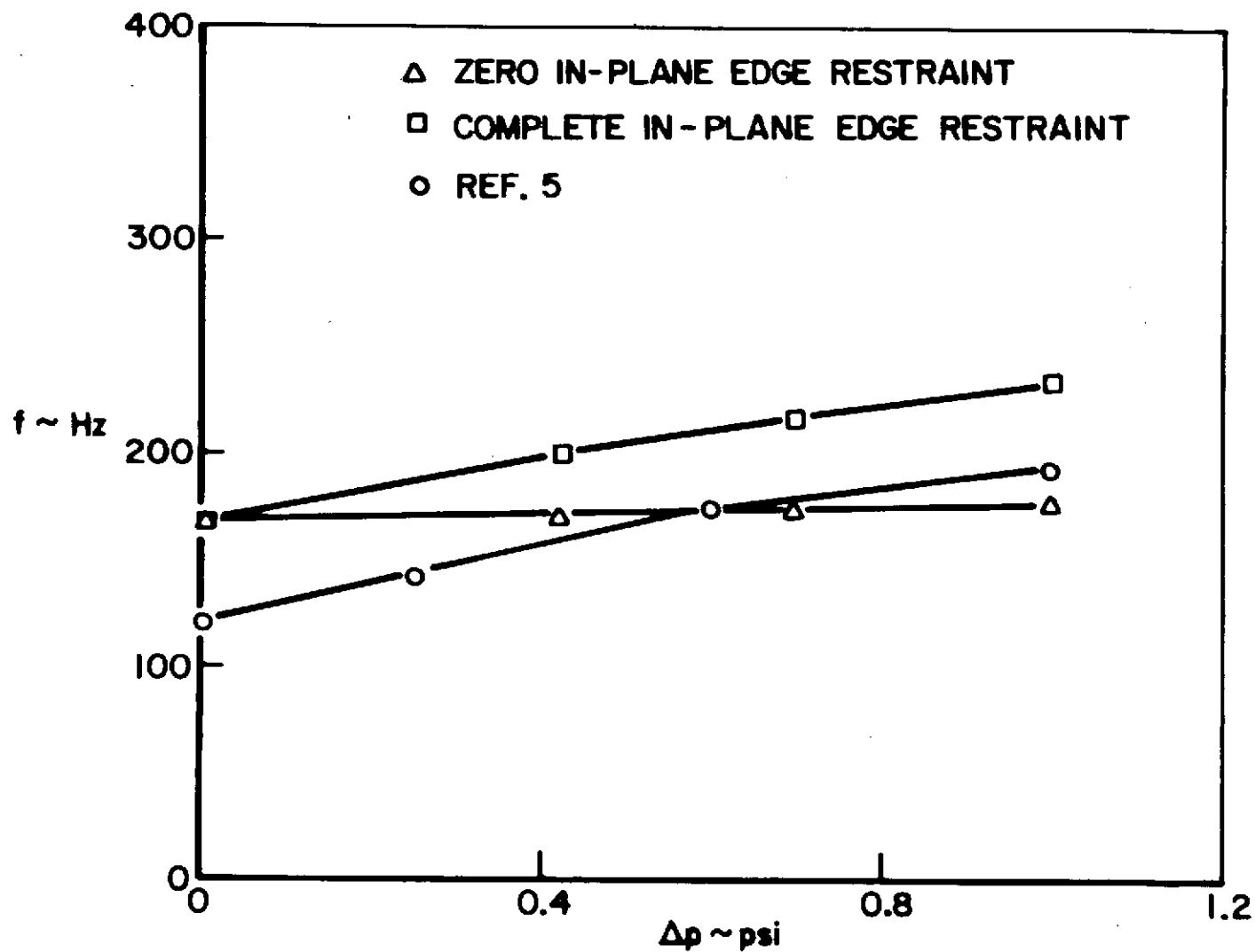
large in-plane loads. In this regard a wind tunnel test program using a carefully constructed high aspect ratio ($a/b < 1$) panel would be very helpful. Stream-wise buckling loads might well be included in the test program, but an extensive set of data should also be collected with little or no in-plane loading present. Such data would be of great help in assessing current theoretical methods without the perplexing but not fundamental difficulties associated with low aspect ratio and panel buckling.

REFERENCES

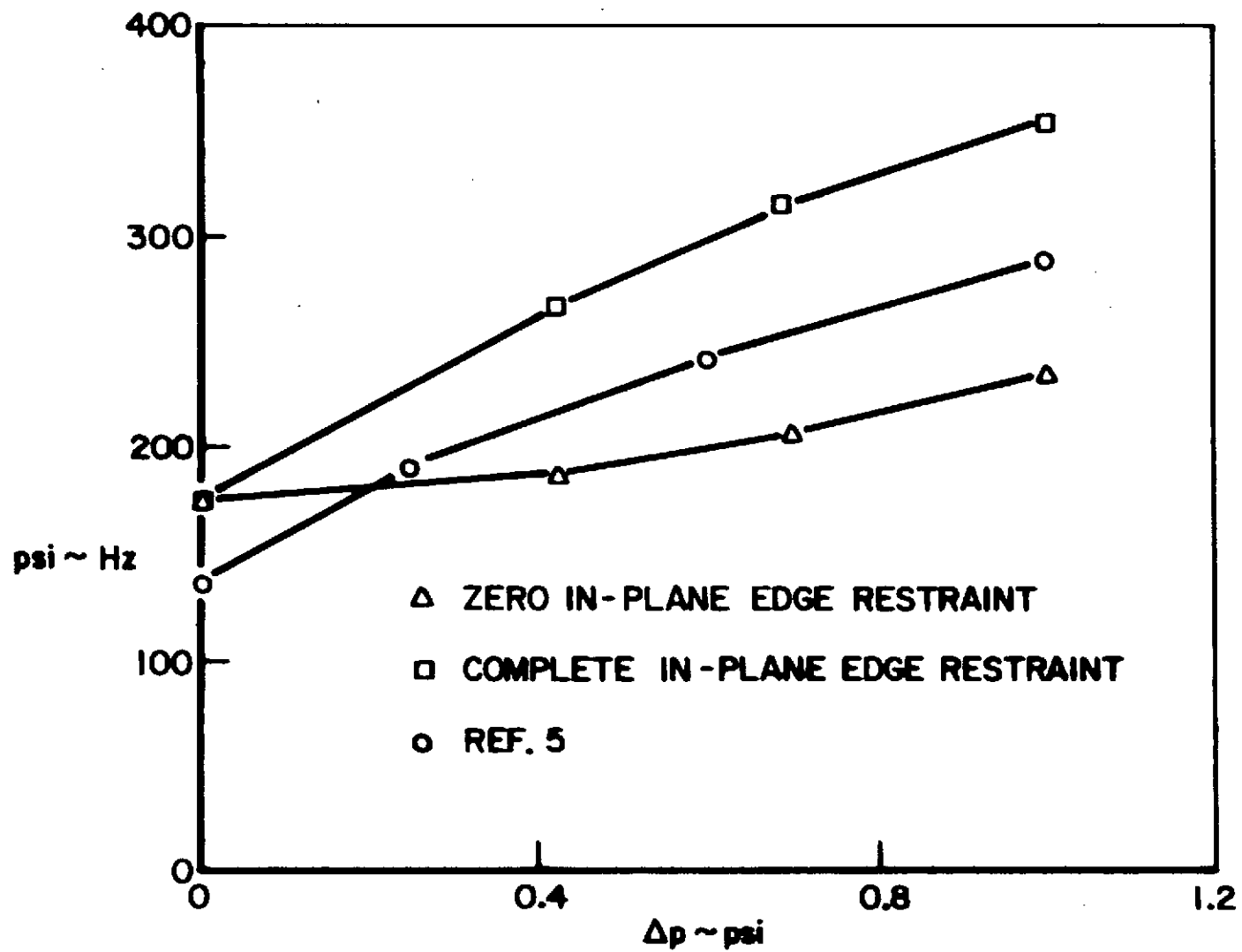
1. Dowell, E. H., "Nonlinear Oscillations of a Fluttering Plate," AIAA Journal, Vol. 4, No. 7, July 1966, pp. 1267-1275.
2. Dowell, E. H., "Nonlinear Oscillations of a Fluttering Plate II," AIAA Journal, Vol. 5, No. 10, 1967, pp. 1856-1862.
3. Ventres, C. S. and Dowell, E. H., "Comparison of Theory and Experiment for Nonlinear Flutter of Loaded Plates," AIAA Journal, Vol. 8, No. 11, 1970, pp. 2022-2030.
4. Ventres, C. S., "Nonlinear Flutter of Clamped Plates," Ph.D. thesis, Department of Aerospace and Mechanical Sciences, Princeton University, 1969.
5. Kappus, H. P., Lemley, C. E. and Zimmerman, N. H., "An Experimental Investigation of High Amplitude Panel Flutter," NASA CR-1837, May 1971.
6. Bolotin, V. V., "Nonconservative Problems of the Theory of Elastic Stability," (The MacMillan Co., New York, 1963) pp. 274-312.
7. Dowell, E. H., "Generalized Aerodynamic Forces on a Flexible Plate Undergoing Transient Motion," Quarterly of Applied Mathematics, Vol. 24, No. 4, 1967, pp. 331-338.
8. Cunningham, H. J., "Flutter Analysis of Flat Rectangular Panels Based on Three-Dimensional Supersonic Unsteady Potential Flow," TR R-256, 1967, NASA.
9. Dowell, E. H., "Generalized Aerodynamic Forces on a Flexible Plate Undergoing Transient Motion in a Shear Flow with an Application to Panel Flutter," AIAA Journal, Vol. 9, No. 5, May 1971, pp. 834-841.
10. Ventres, C. S., "Flutter of a Buckled Plate Exposed to a Static Pressure Differential," AIAA Journal, Vol. 9, No. 5, May 1971, pp. 958-960.

LIST OF FIGURES

Figure 1	Effect of Δp on Frequency Spectra 1st Mode
Figure 2	Effect of Δp on Frequency Spectra 2nd Mode
Figure 3	Effect of Δp on Frequency Spectra 6th Mode
Figure 4	Frequency of Ninth Mode vs In-Plane Load
Figure 5	Variation of Onset Dynamic Pressure with Mach Number
Figure 6	Variation of Onset Dynamic Pressure with Mach Number
Figure 7	Effect of Damping on Flutter Onset Frequencies
Figure 8	Variation of Flutter Onset Dynamic Pressure with Compressive Edge Load
Figure 9	Variation of Flutter Onset Dynamic Pressure with Compressive Edge Load
Figure 10	Effect of Δp on Flutter Onset Dynamic Pressure (Different Boundary Conditions)
Figure 11	Effect of Δp on Flutter Onset Dynamic Pressure (with Variation in N_x)
Figure 12	Effect on N_x on Flutter Onset Dynamic Pressure
Figure 13	Effect of Δp on Flutter Onset
Figure 14	Panel Motion During Flutter
Figure 15	Panel Oscillatory Displacement During Flutter
Figure 16	Panel Bending Stress and Displacement
Figure 17	Oscillatory Bending Stress of a Buckled Panel During Flutter
Figure 18a	Oscillatory Bending Stress During Flutter
Figure 18b	Maximum Bending Stress During Flutter
Figure 19a	Oscillatory Bending Stress During Flutter
Figure 19b	Maximum Bending Stress During Flutter
Figure 20a	Oscillatory Axial Stress During Flutter
Figure 20b	Maximum Axial Stress During Flutter
Figure 21a	Oscillatory Axial Stress During Flutter
Figure 21b	Maximum Axial Stress During Flutter

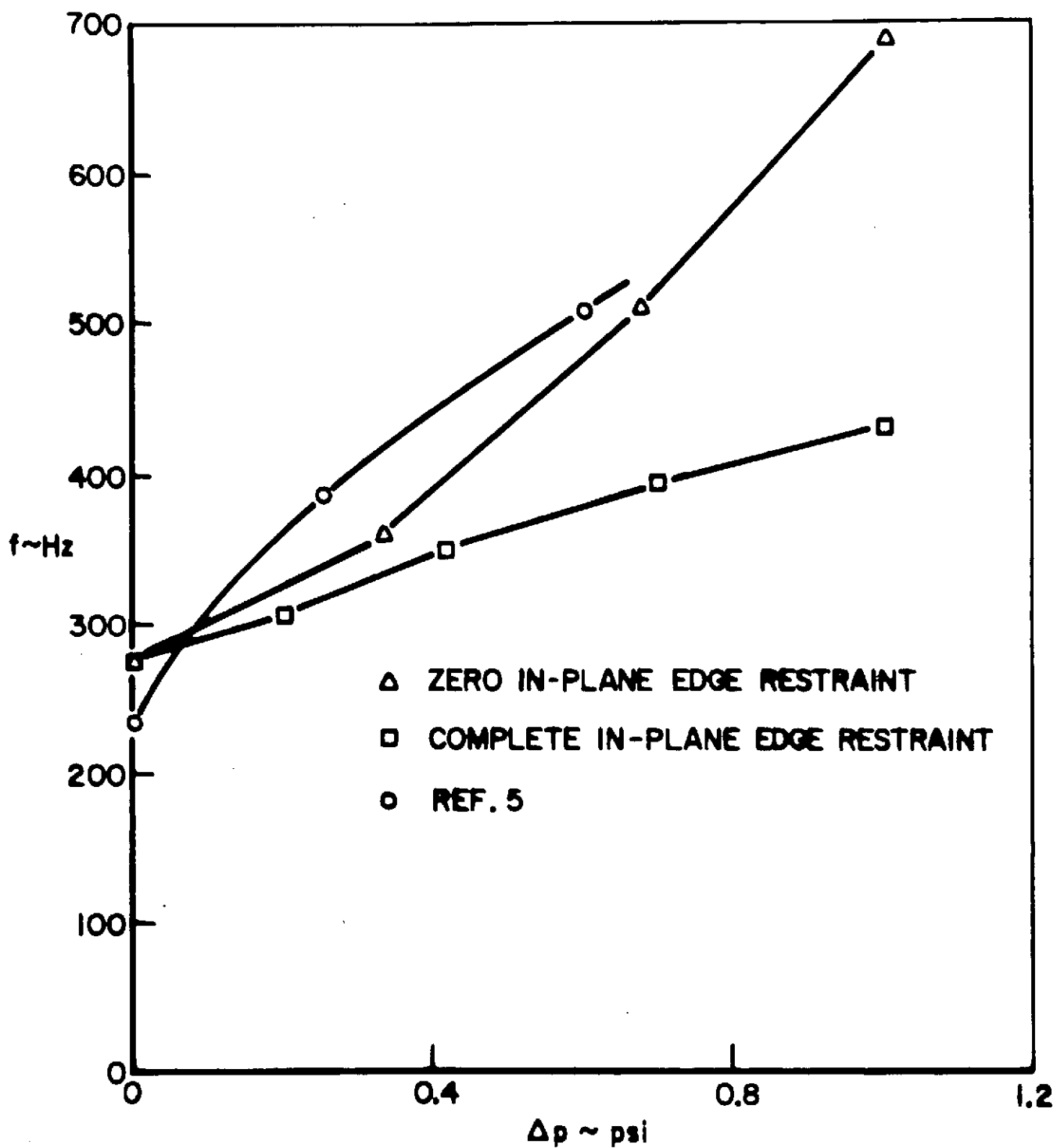


EFFECT OF Δp ON FREQUENCY
SPECTRA 1st MODE



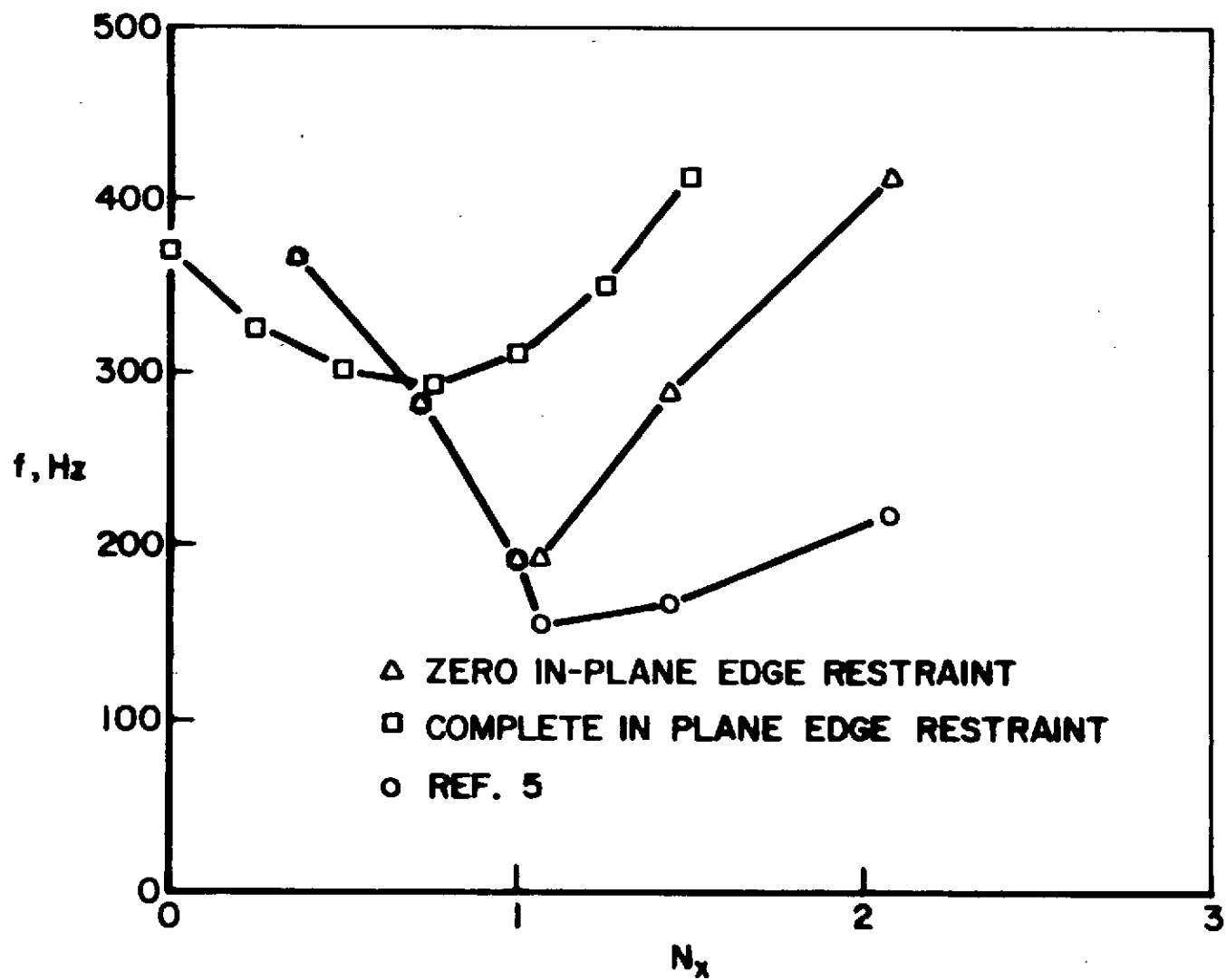
EFFECT OF Δp ON FREQUENCY
SPECTRA 2nd MODE

FIGURE 2

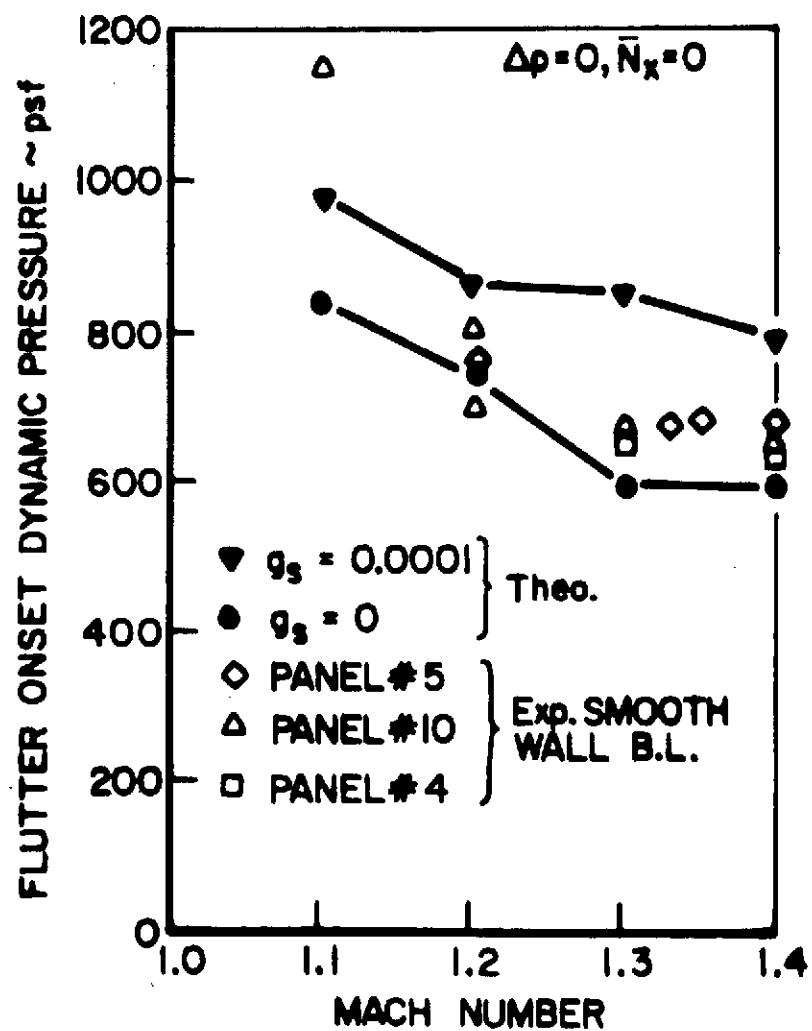


EFFECT OF Δp ON FREQUENCY
SPECTRA 6th MODE

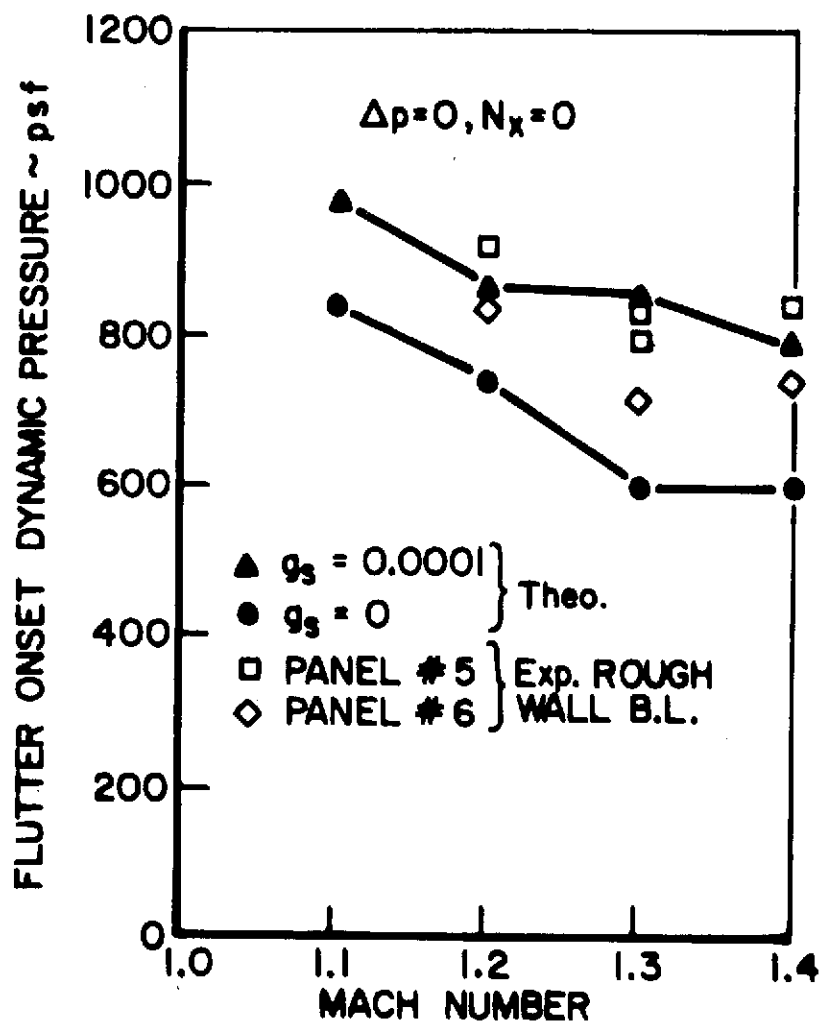
FIGURE 3



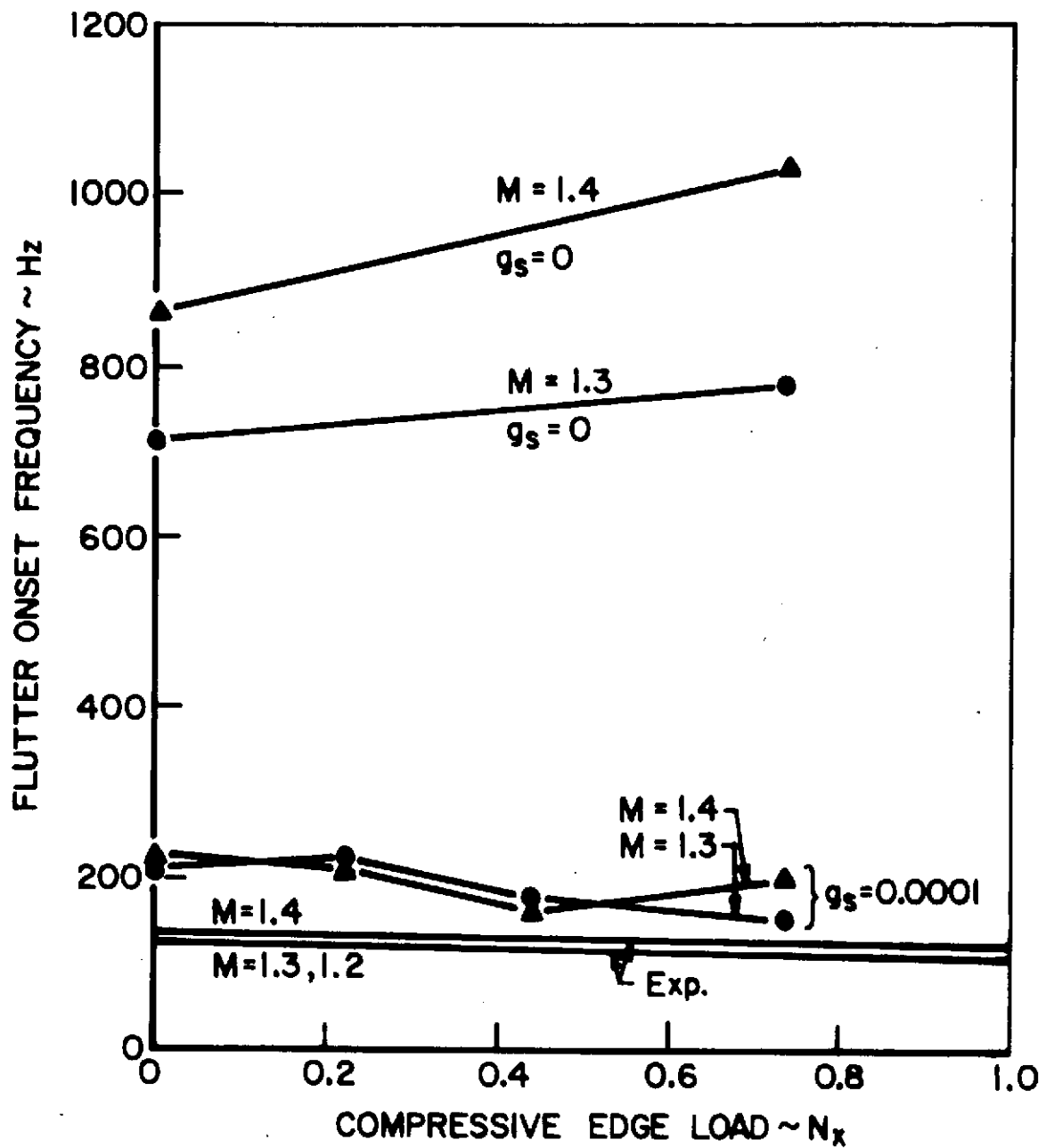
FREQUENCY OF NINTH MODE
vs IN-PLANE LOAD



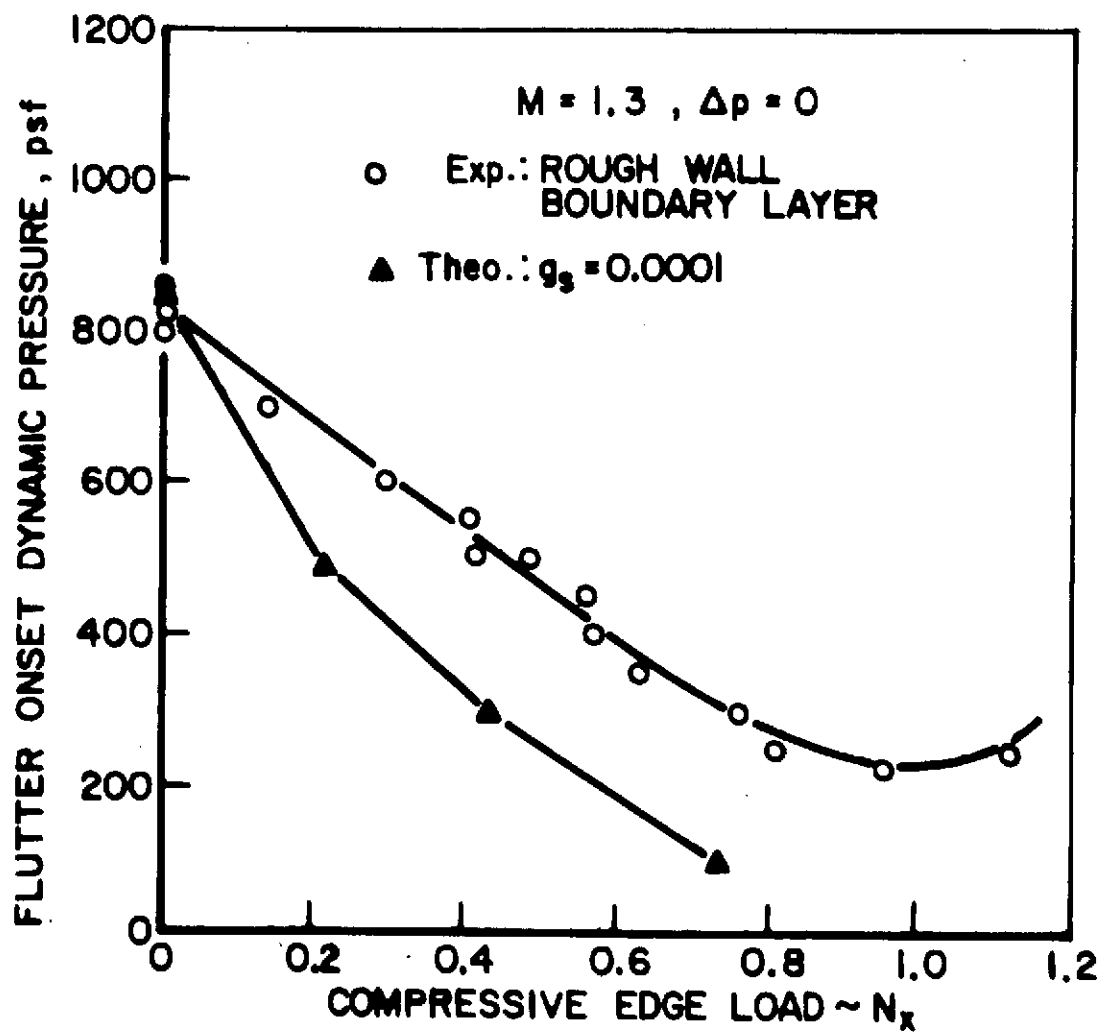
VARIATION OF ONSET DYNAMIC PRESSURE
WITH MACH NUMBER



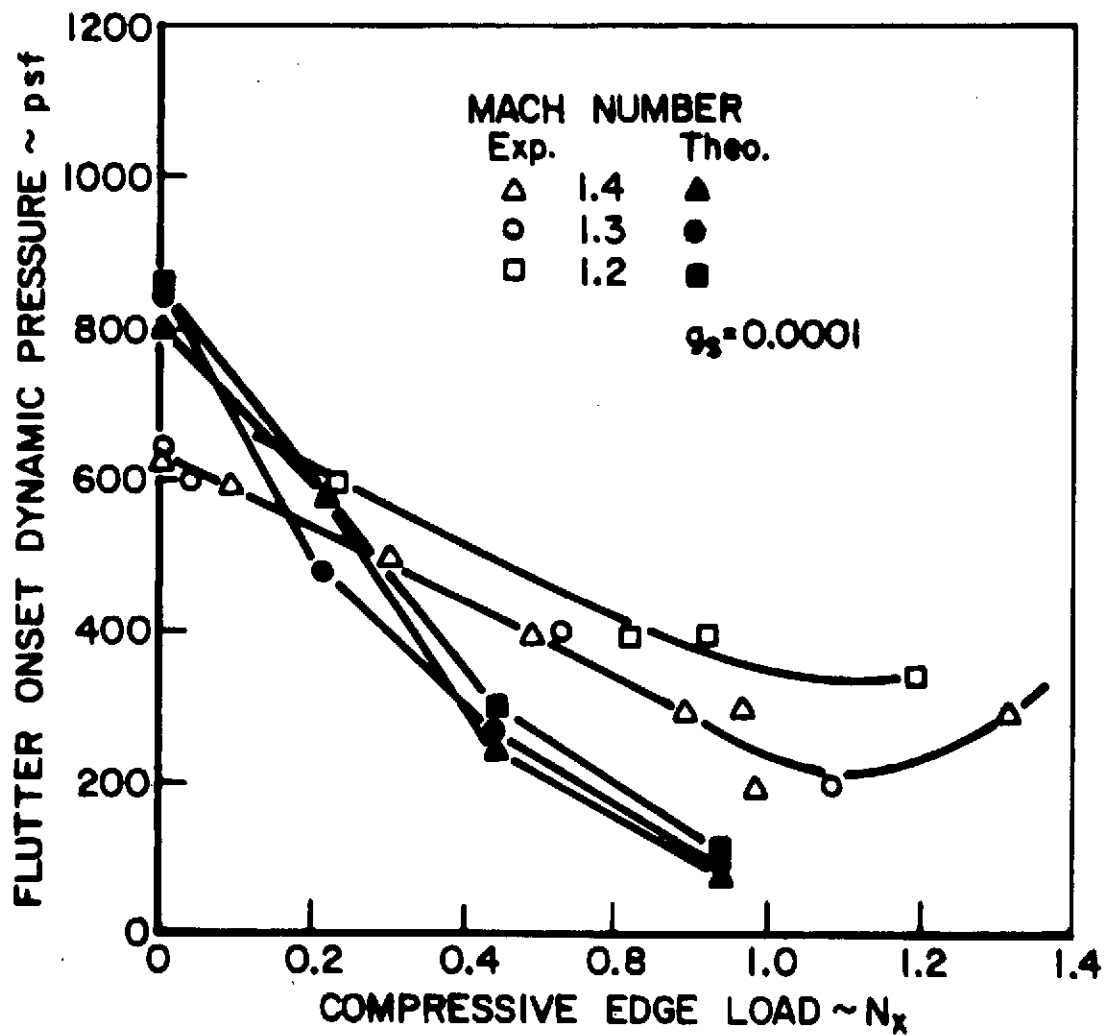
VARIATION OF ONSET DYNAMIC PRESSURE
WITH MACH NUMBER



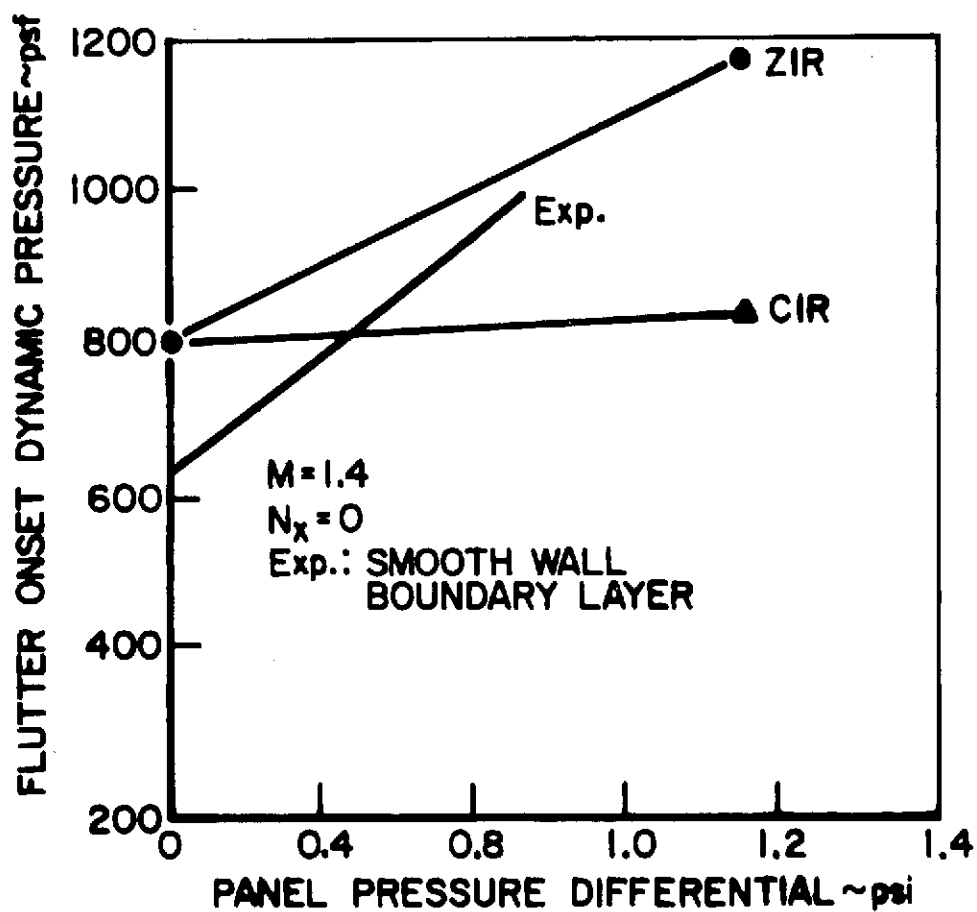
EFFECT OF DAMPING ON FLUTTER ONSET FREQUENCIES



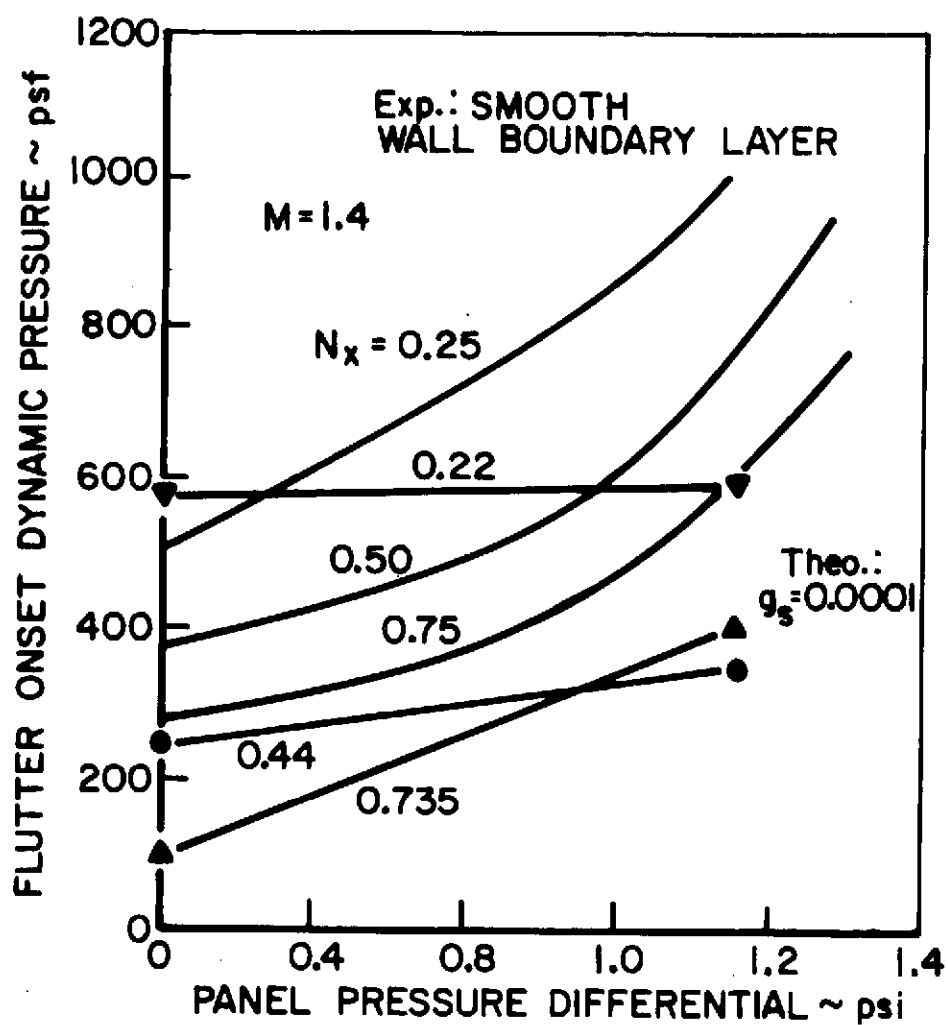
VARIATION OF FLUTTER ONSET DYNAMIC PRESSURE
WITH COMPRESSIVE EDGE LOAD



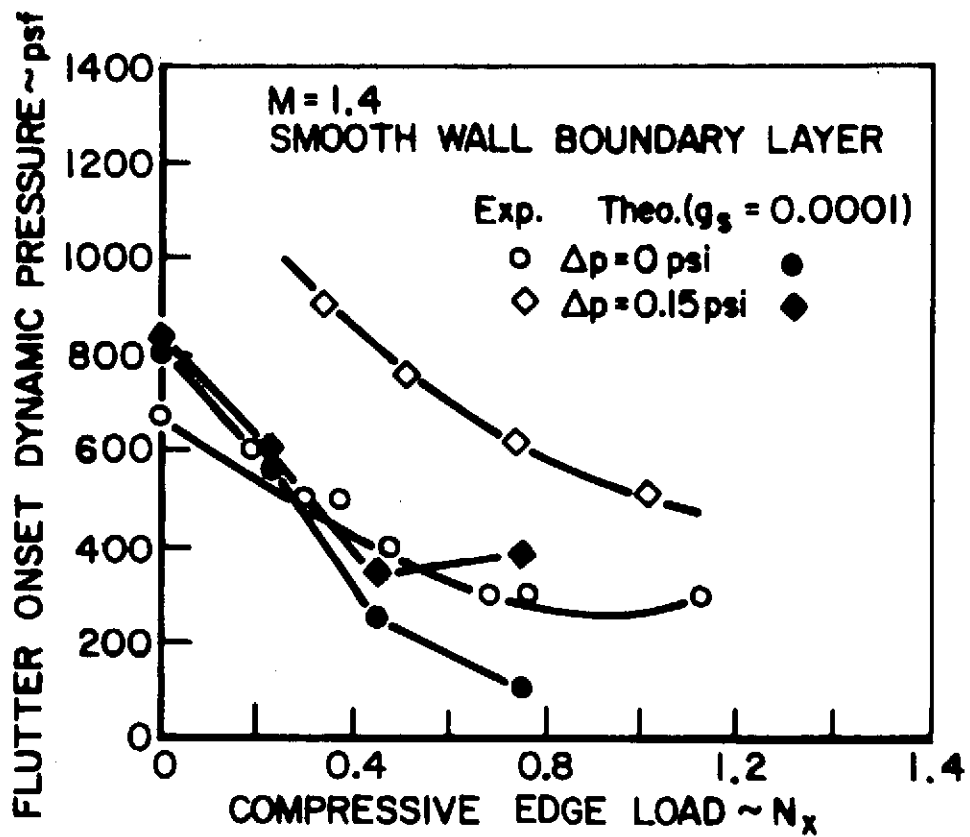
VARIATION OF FLUTTER ONSET DYNAMIC PRESSURE
WITH COMPRESSIVE EDGE LOAD



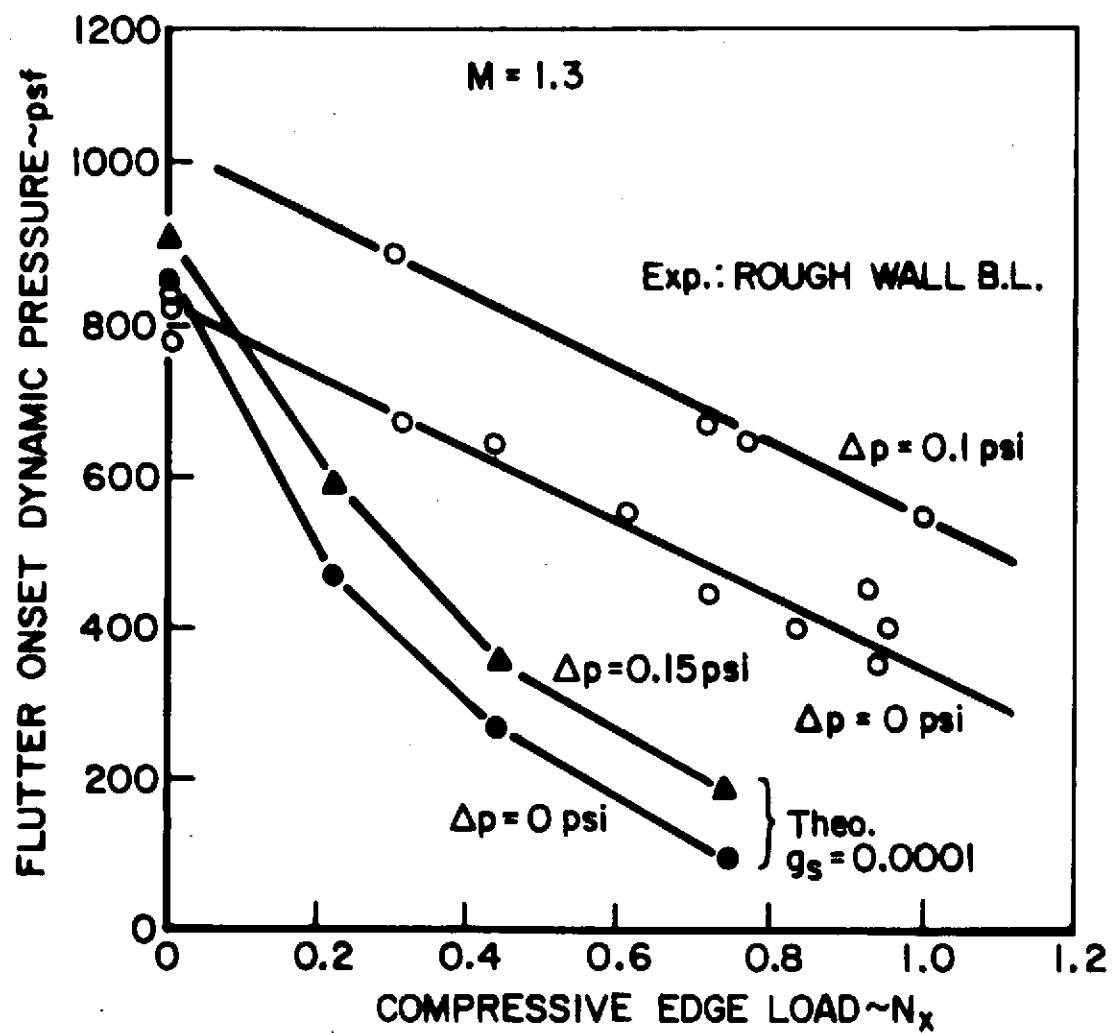
EFFECT OF Δp ON FLUTTER ONSET DYNAMIC PRESSURE (DIFFERENT BOUNDARY CONDITIONS)



EFFECT OF Δp ON FLUTTER ONSET DYNAMIC PRESSURE (WITH VARIATION IN N_x)

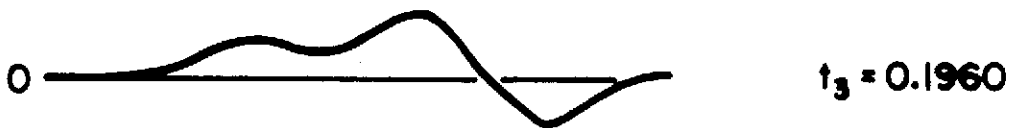
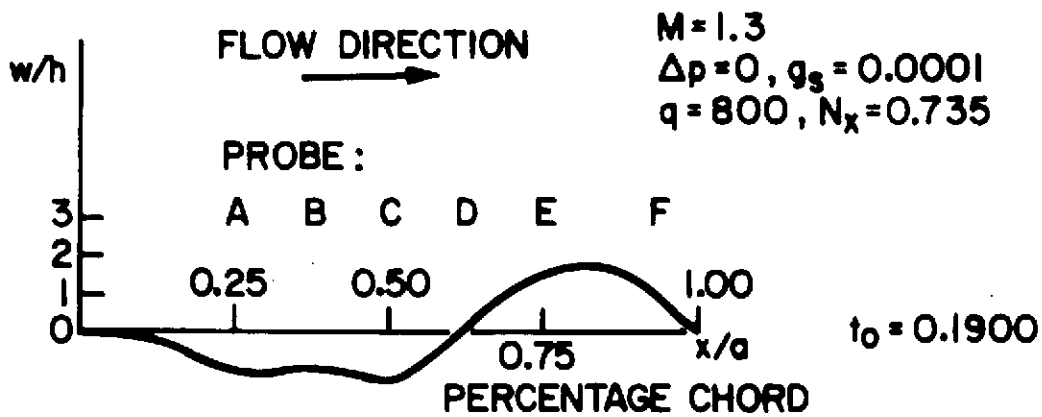


EFFECT OF N_x ON FLUTTER ONSET DYNAMIC PRESSURE



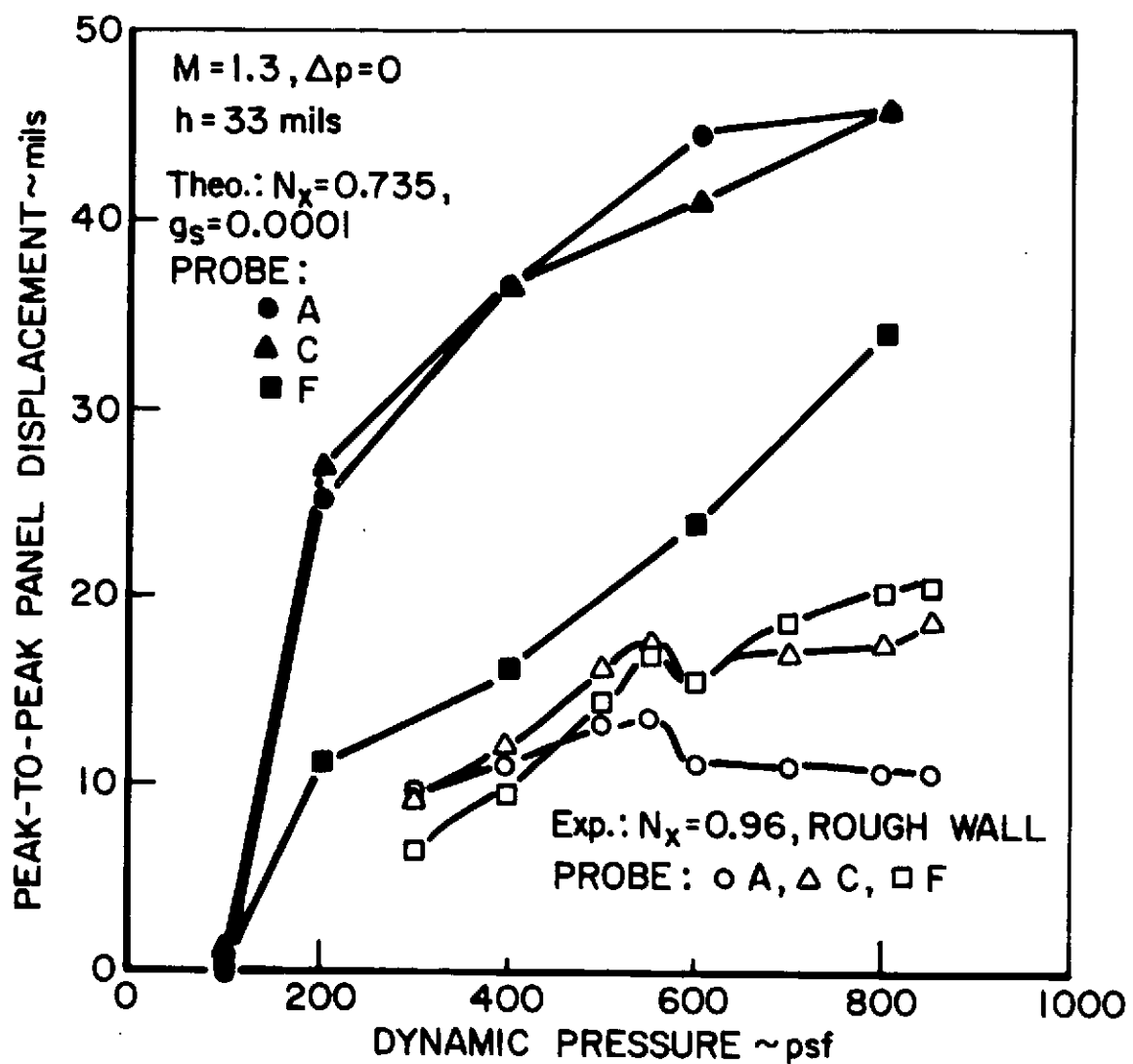
EFFECT OF Δp ON FLUTTER ONSET

PANEL DISPLACEMENT

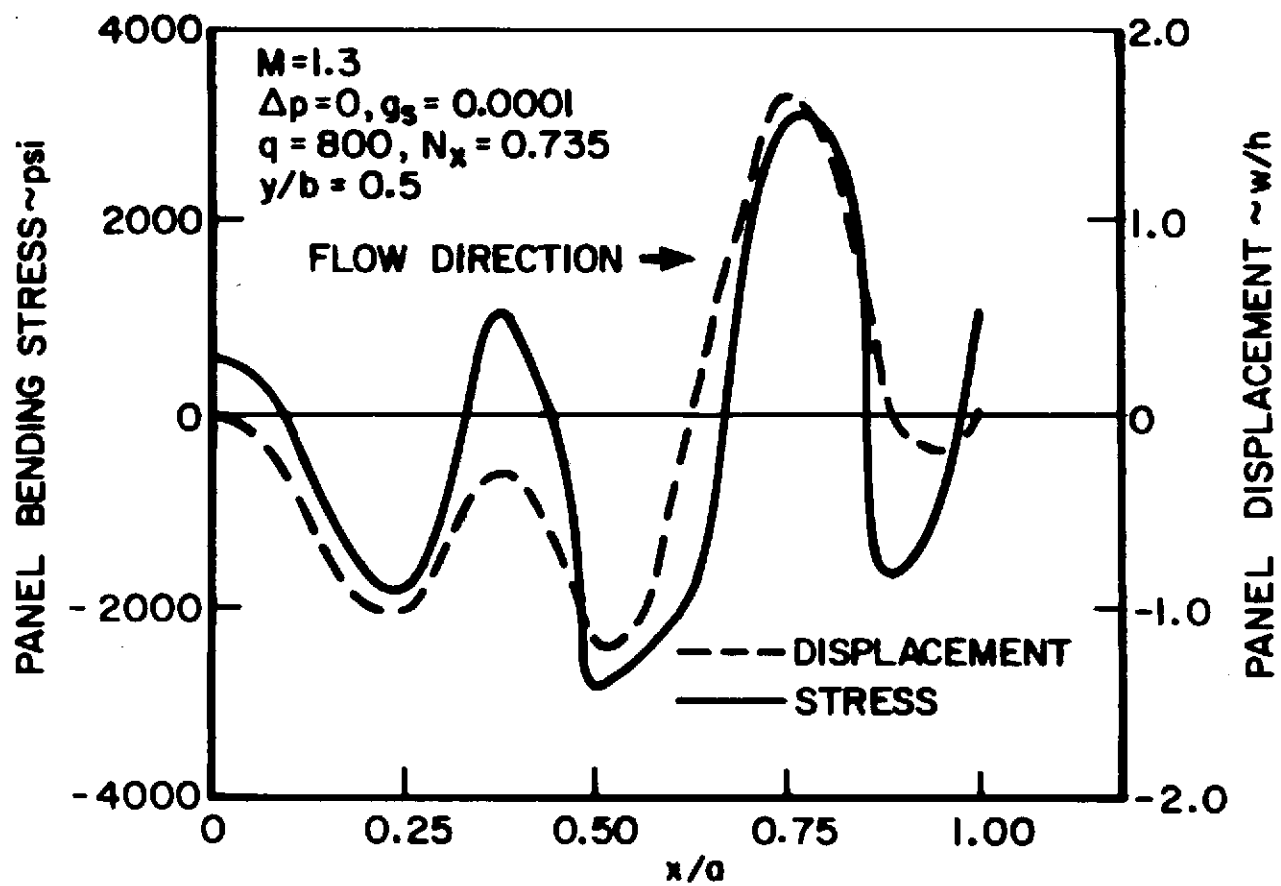


PANEL MOTION DURING FLUTTER

FIGURE 14

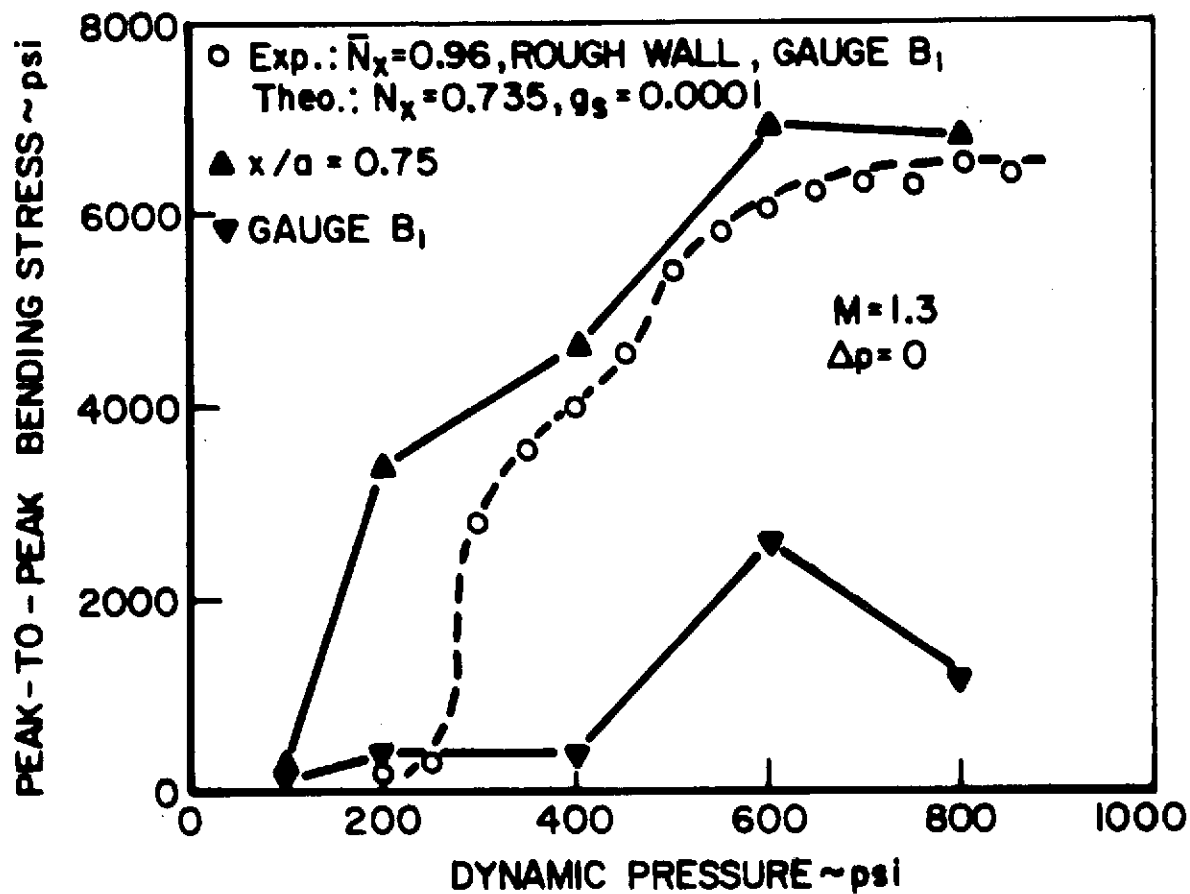


PANEL OSCILLATORY DISPLACEMENT DURING FLUTTER

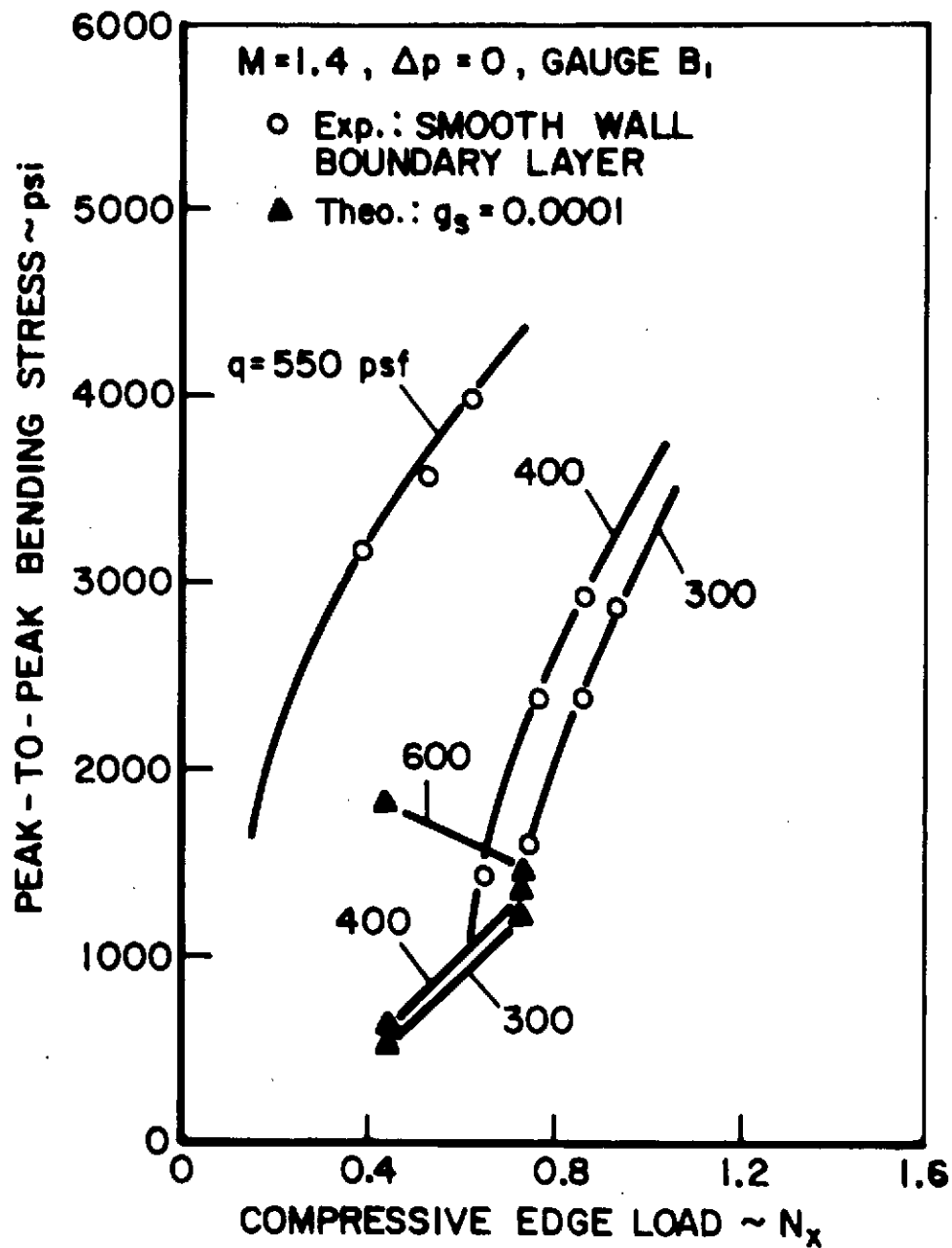


PANEL BENDING STRESS AND DISPLACEMENT

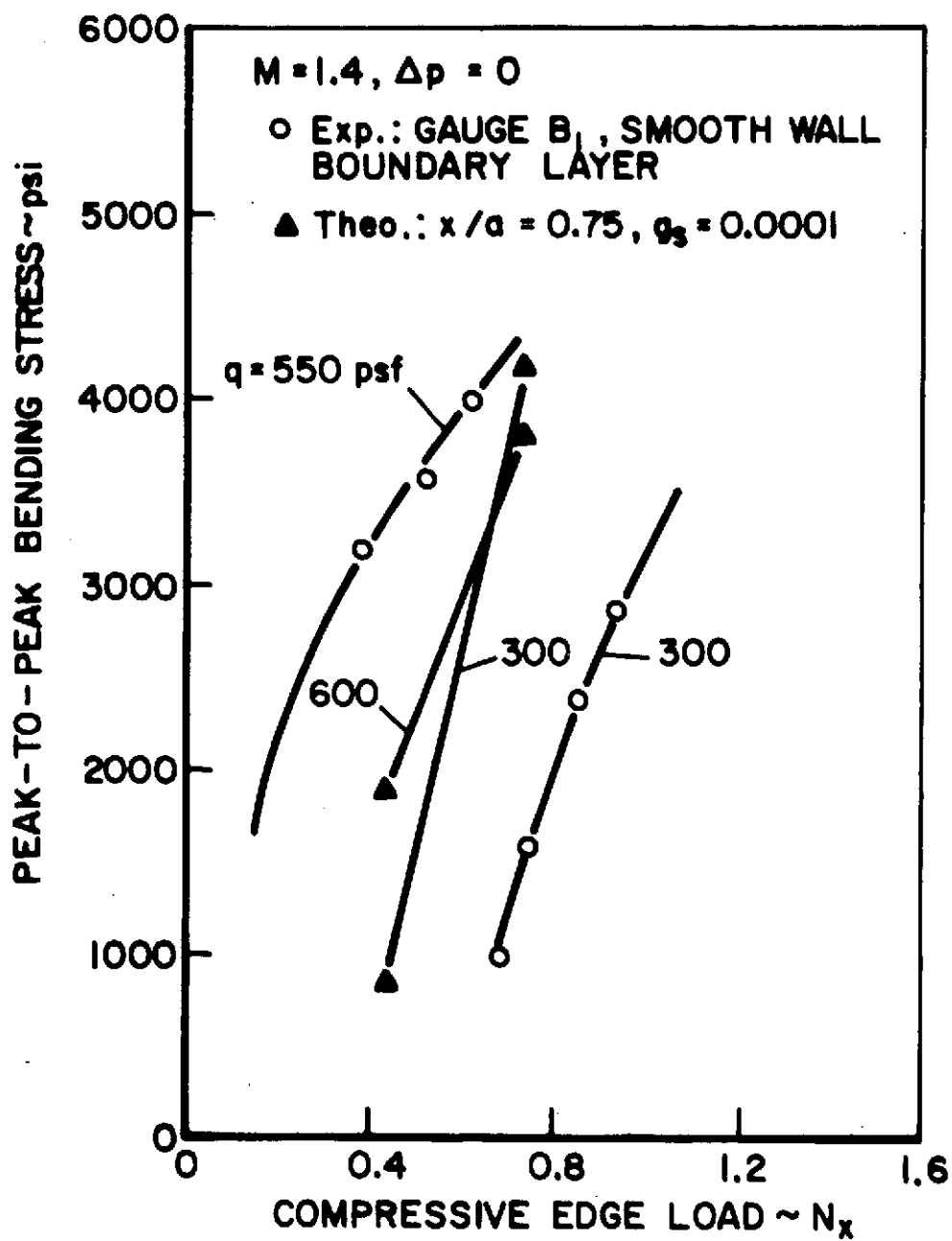
FIGURE 16



OSCILLATORY BENDING STRESS OF A BUCKLED PANEL DURING FLUTTER

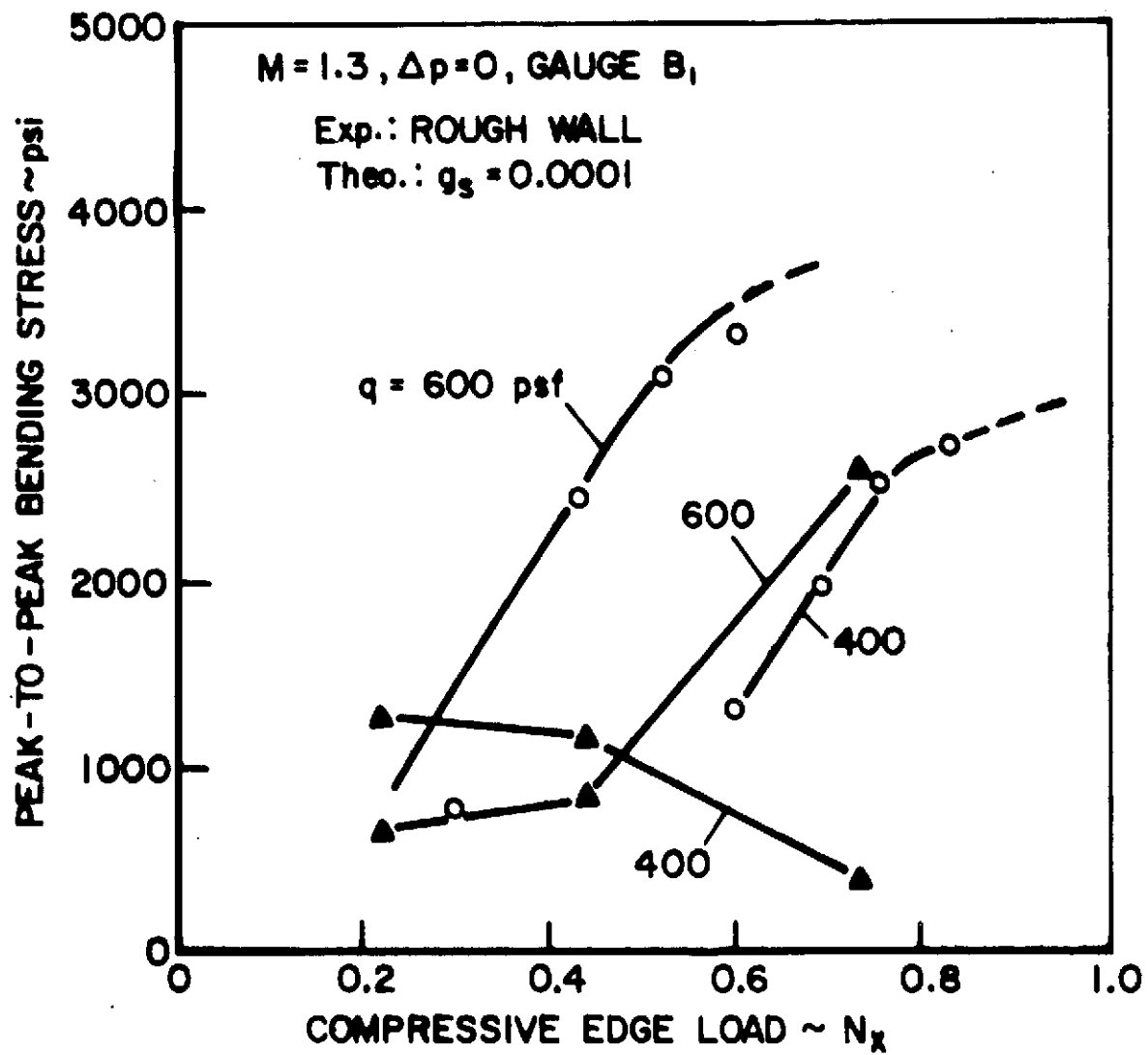


OSCILLATORY BENDING STRESS DURING FLUTTER

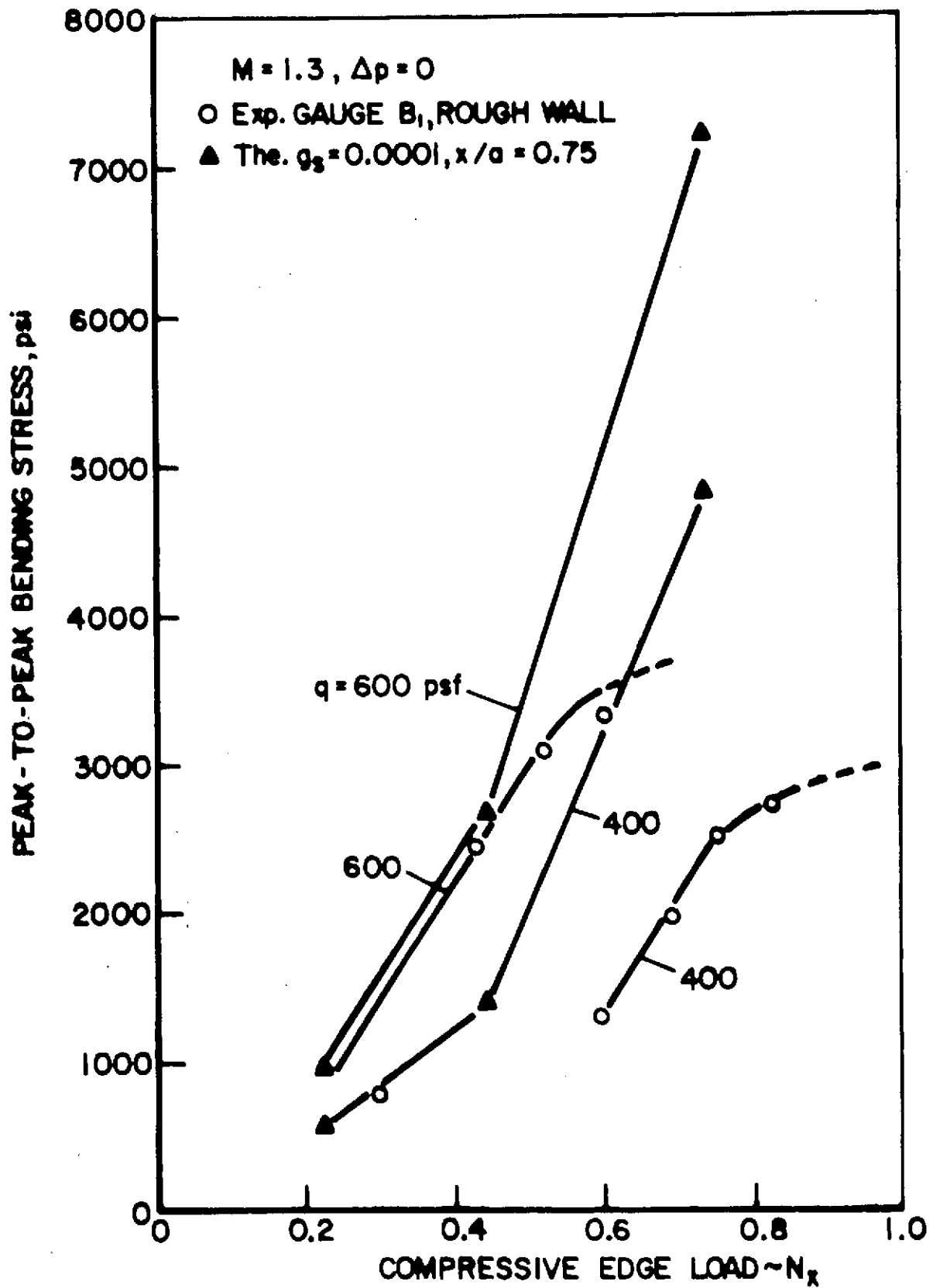


MAXIMUM BENDING STRESS DURING FLUTTER

FIGURE 18b

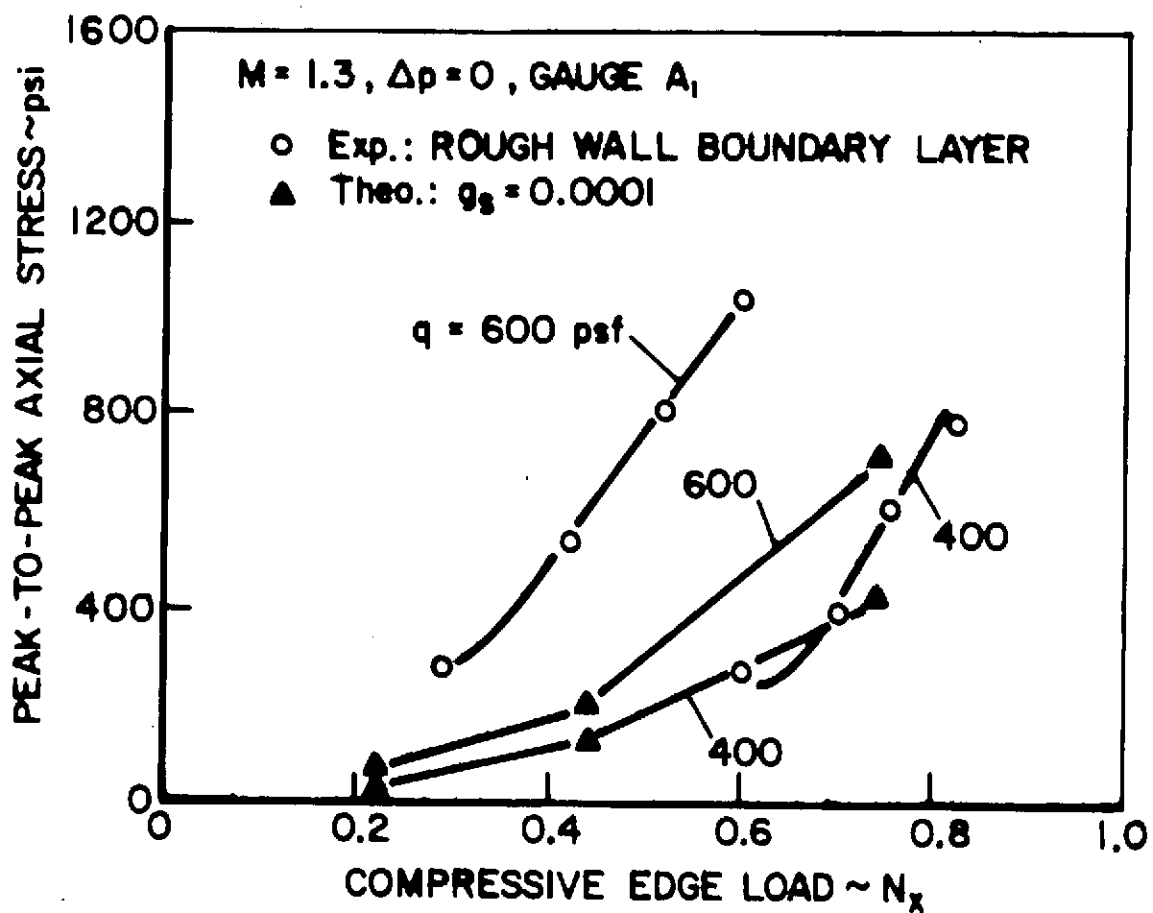


OSCILLATORY BENDING STRESS DURING FLUTTER



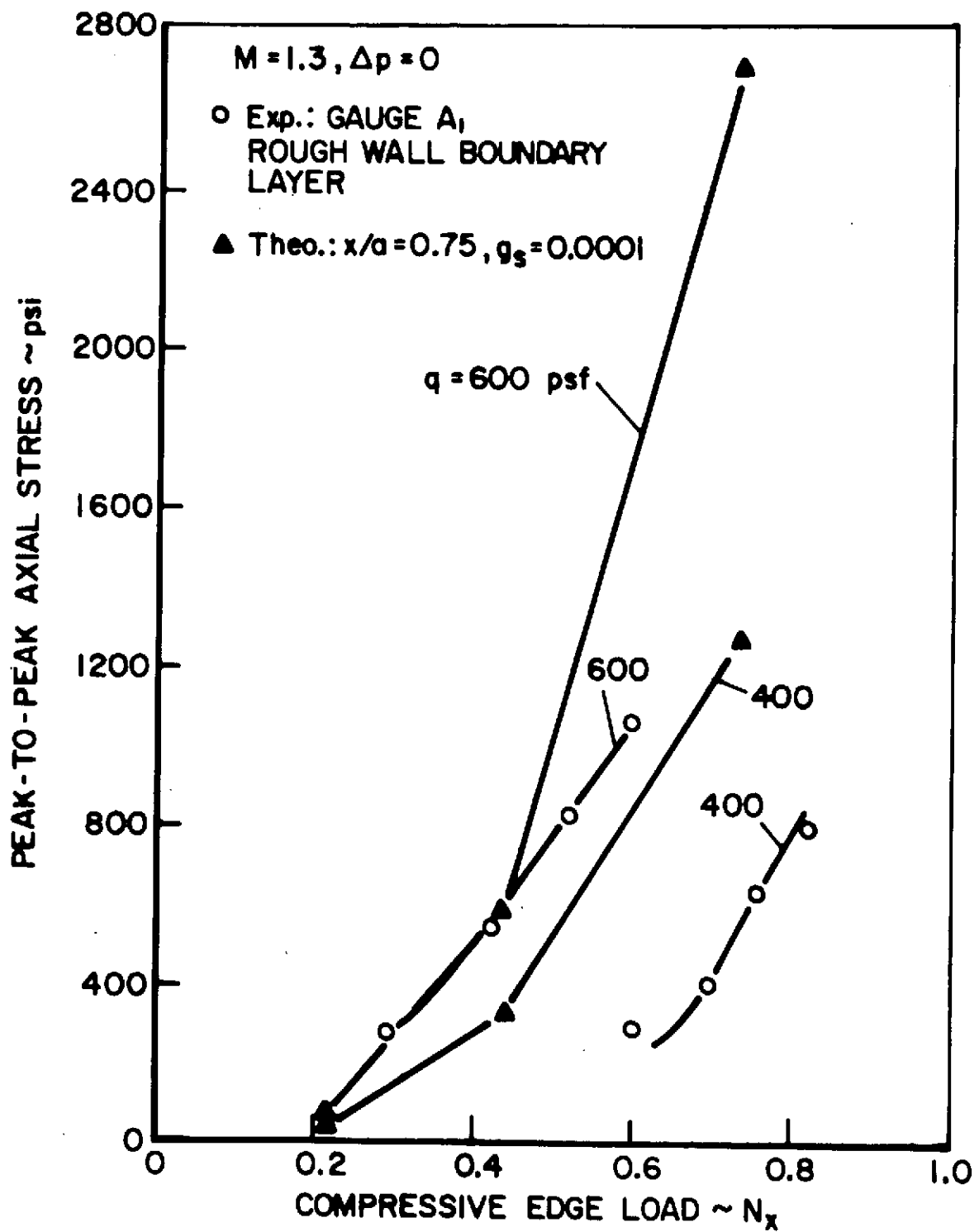
MAXIMUM BENDING STRESS DURING FLUTTER

FIGURE 19 b



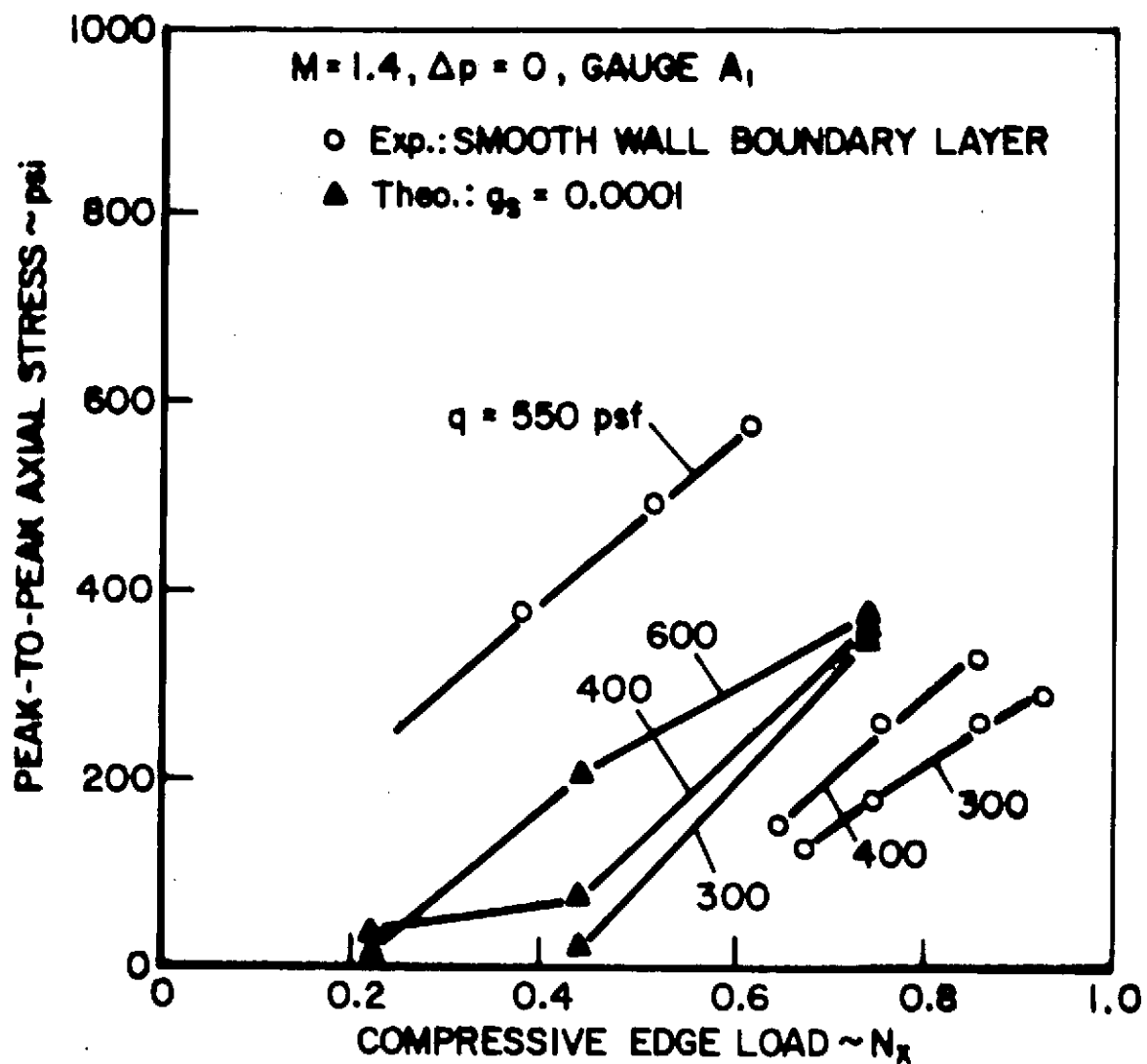
OSCILLATORY AXIAL STRESS DURING FLUTTER

FIGURE 20a



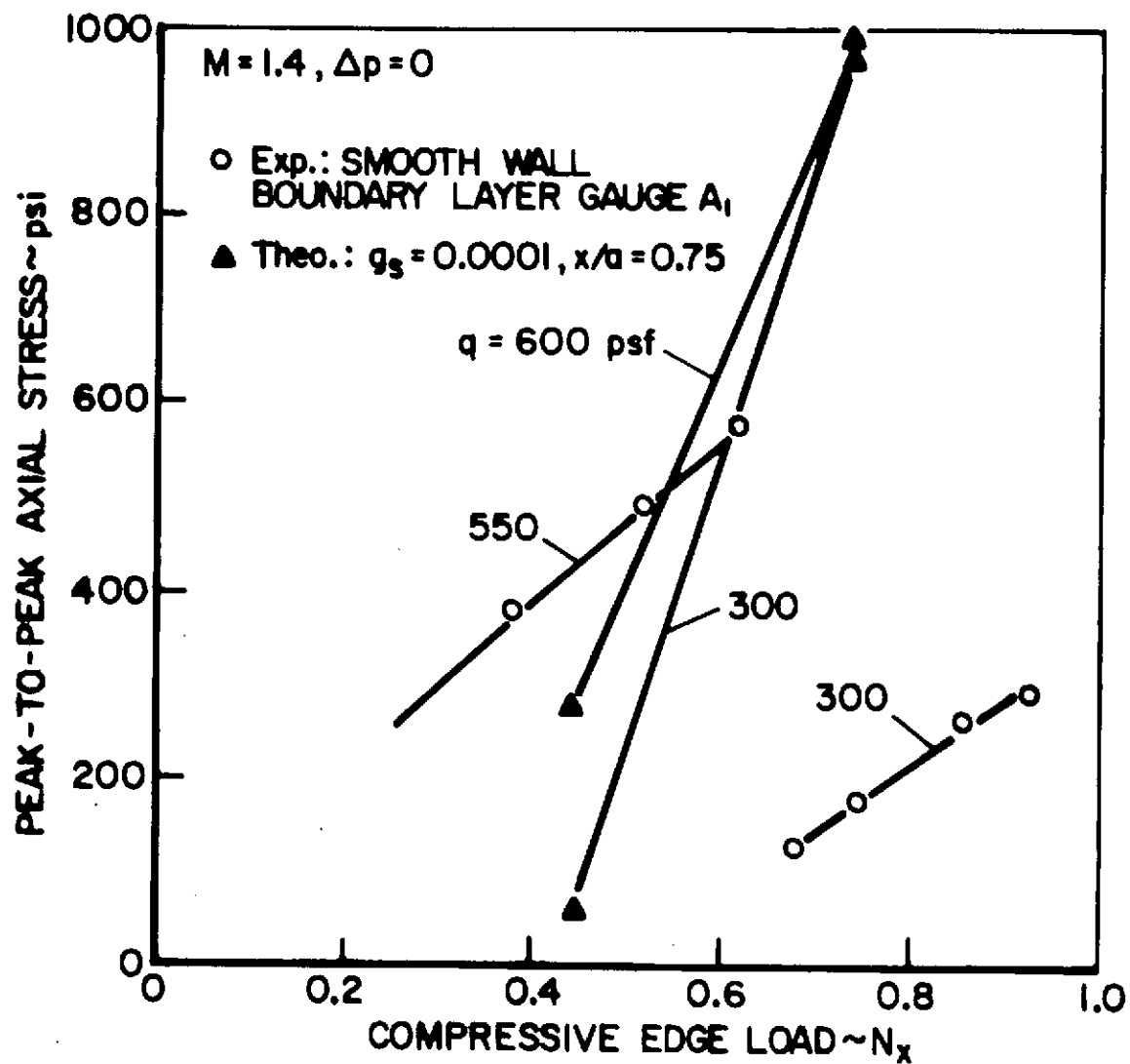
MAXIMUM AXIAL STRESS DURING FLUTTER

FIGURE 20b



OSCILLATORY AXIAL STRESS DURING FLUTTER

FIGURE 21a



MAXIMUM AXIAL STRESS DURING FLUTTER

FIGURE 21b

APPENDIX

Listing of Computer Programs

```

COMPILER OPTIONS - NAME= MAIN,OPT=02,LINECNT=58,SIZE=0000K,
SOURCE,EBCDIC,NOLIST,NODECK,LOAD,MAP,NOEDIT,ID,NOXREF
C    PROGRAM TO COMPUTE NONLINEAR TERMS (COUPLING BETWEEN
C    IN-PLANE STRETCHING AND OUT OF PLANE BENDING) FOR CLAMPED
C    PLATE WITH COMPLETE IN-PLANE EDGE RESTRAINT
C    AB=PLATE LENGTH/WIDTH RATIO,NU=POISSON'S RATIO
C    NV = # OF MODES
ISN 0002    REAL NU
ISN 0003    REAL II
ISN 0004    DIMENSION B(12,12,12,12)
ISN 0005    DNA(K) = (FLOAT(K)**2+16.*AB2)**2
ISN 0006    DNB(K) = (FLOAT(K)**2+4.*AB2)**2
ISN 0007    CSS(K,L,M) = .5*(CC(K,L-M)-CC(K,L+M))
ISN 0008    CCC(K,L,M) = .5*(CC(K,L-M) + CC(K,L+M))
ISN 0009    GG(K,L,M) = CCC(K-1,L-1,M) -CCC(K-1,L+1,M) -CCC(K+1,L-1,M)
ISN 0010    1 +CCC(K+1,L+1,M)
ISN 0011    HH(K,L,M) = -PI2*FLOAT(L-1)**2*(CCC(K-1,L-1,M)
ISN 0012    1 -CCC(K+1,L-1,M))
ISN 0013    2 + PI2*FLOAT(L+1)**2*(CCC(K-1,L+1,M) -CCC(K+1,L+1,M))
ISN 0014    II(K,L,M) = -PI*FLOAT(L-1)*(CSS(K-1,L-1,M) -CSS(K+1,L-1,M))
ISN 0015    1 + PI*FLOAT(L+1)*(CSS(K-1,L+1,M) -CSS(K+1,L+1,M))
ISN 0016    1    FORMAT (1H0)
ISN 0017    2    FORMAT (1H1)
ISN 0018    PI = 3.14159
ISN 0019    PI2 = PI*PI
ISN 0020    PI3 = PI2*PI
ISN 0021    PI4 = PI3*PI
ISN 0022    READ (5,110) AB,NU
ISN 0023    110    FORMAT(4E10.3)
ISN 0024    WRITE(6,1101) AB,NU
ISN 0025    1101    FORMAT(2E12.3)
ISN 0026    WRITE (6,1)
ISN 0027    READ(5,120) NV
ISN 0028    WRITE(6,120) NV
ISN 0029    120    FORMAT(I5)
ISN 0030    WRITE (6,1)
ISN 0031    AB2 = AB**2
ISN 0032    AB4 = AB**4
ISN 0033    X = 1.0E-12
ISN 0034    DO 42 M = 1,NV
ISN 0035    DO 42 N = 1,NV
ISN 0036    MA = M-N
ISN 0037    MB = M-N-2
ISN 0038    MC = M-N+2
ISN 0039    MD = M+N
ISN 0040    ME = M+N-2
ISN 0041    MF = M+N+2
ISN 0042    RM = M
ISN 0043    RN = N
ISN 0044    RMA = MA
ISN 0045    RMB = MB
ISN 0046    RMC = MC
ISN 0047    RMD = MD
ISN 0048    RME = ME
ISN 0049    RMF = MF
ISN 0050    BA = -2.*(RM*RMD+2.)/DNA(MA)

```

```

ISN 0047      BB = (RM-1.) * RMJ / DNA (MB)
ISN 0048      BC = (RM+1.) * RMJ / DNA (MC)
ISN 0049      BD = 2. * (RM * RMA + 2.) / DNA (MD)
ISN 0050      BE = - (RM-1.) * RMA / DNA (ME)
ISN 0051      BF = - (RM+1.) * RMA / DNA (MF)
ISN 0052      BG = 4. * (RM**2+1.) / DNB (MA)
ISN 0053      BH = -2. * (RM-1.) **2 / DNB (MB)
ISN 0054      BK = -2. * (RM+1.) **2 / DNB (MC)
ISN 0055      BL = -4. * (RM**2+1.) / DNB (MD)
ISN 0056      BM = 2. * (RM-1.) **2 / DNB (ME)
ISN 0057      BN = 2. * (RM+1.) **2 / DNB (MF)
ISN 0058      BP = -2. * RM / (R1A**3+X)
ISN 0059      BQ = (RM-1.) / (R1B**3+X)
ISN 0060      BR = (RM+1.) / (R1C**3+X)
ISN 0061      BS = 2. * RM / RMD**3
ISN 0062      BT = - (RM-1.) / (RME**3+X)
ISN 0063      BU = - (RM+1.) / RMF**3
ISN 0064      DO 42 I = 1, NV
ISN 0065      DO 42 K = 1, NV
ISN 0066      IODD = I+K+M+N
ISN 0067      IF (MOD (IODD, 2) .NE. 0) GO TO 38
ISN 0069      BAA = (BA-BG) * HH (I, K, MA) + (BB-BH) * HH (I, K, MB) +
1 (BC-BK) * HH (I, K, MC) + (BD-BL) * HH (I, K, MD) +
2 (BE-BM) * HH (I, K, ME) + (BF-BN) * HH (I, K, MF)
ISN 0070      BAA = -43. * (1.-NU**2) * AB2 * PI2 * EAA
ISN 0071      BBB = RMA * (BA-BG) * II (I, K, MA) + RMB * (BB-BH) * II (I, K, MB)
1 + RMC * (BC-BK) * II (I, K, MC) + RMD * (BD-BL) * II (I, K, MD) +
2 RME * (BE-BM) * II (I, K, ME) + RMF * (BF-BN) * II (I, K, MF)
ISN 0072      BBB = -24. * (1.-NU**2) * AB2 * PI3 * BBB
ISN 0073      BCC = RMA**2 * (BA-2. * BG+2. * BP) * GG (I, K, MA)
1 + RMB**2 * (BB-2. * BH+2. * BQ) * GG (I, K, MB)
3 + RMC**2 * (BC-2. * BK+2. * BR) * GG (I, K, MC)
4 + RMD**2 * (BD-2. * BL+2. * BS) * GG (I, K, MD)
5 + RME**2 * (BE-2. * BM+2. * BT) * GG (I, K, ME)
6 + RMF**2 * (BF-2. * BN+2. * BU) * GG (I, K, MF)
ISN 0074      BCC = 12. * (1.-NU**2) * AB2 * PI4 * BCC
ISN 0075      B (I, K, M, N) = -A32 * (BAA-2. * EBB+BCC)
ISN 0076      GO TO 42
ISN 0077      38 B (I, K, M, N) = 0.
ISN 0078      42 B (K, I, M, N) = B (I, K, M, N)
C      WRITE NONLINEAR TERMS ONTO TAPE
ISN 0079      WRITE (10) B
ISN 0080      ENDFILE 10
ISN 0081      DO 45 I = 1, NV
ISN 0082      DO 45 J = 1, NV
ISN 0083      DO 45 K = 1, NV
ISN 0084      45 WRITE (5, 47) (B (I, J, K, L), L = 1, NV)
ISN 0085      47 FORMAT (10E12.3)
ISN 0086      STOP
ISN 0087      END

```


COMPILER OPTIONS - NAME= MAIN,OPT=02,LINECNT=58,SIZE=0000K,
SOURCE,EBCDIC,NOLIST,NODECK,LOAD,MAP,NOEDIT,ID,NOXREF

```
ISN 0002      FUNCTION CC(K,M)
ISN 0003      CC = 0.
ISN 0004      IF(K.EQ.M) CC = CC+.5
ISN 0006      IF(K.EQ.-M) CC = CC+.5
ISN 0008      RETURN
ISN 0009      END
```

```

C      PROGRAM TO COMPUTE NONLINEAR TERMS (COUPLING
C      BETWEEN IN-PLANE STRETCHING AND OUT OF PLANE BENDING)
C      FOR PLATES WITH ZERO IN-PLANE EDGE RESTRAINT
C      AB=PLATE LENGTH/WIDTH RATIO, NU=POISSON'S RATIO,
C      NV=# OF MODES
0001      REAL NU
0002      DIMENSION B(12,12,12,12)
0003      DIMENSION AA(30,3,30,3),V(14,30,3,14),G(30,3,14,14)
0004      DIMENSION AM(90,90),AMW(90,90)
0005      DIMENSION AVW(180)
0006      REAL*8 AM,AMW
0007      REAL*8 AVW
0008      CSS(K,L,M) = .5*(CC(K,L-M) - CC(K,L+M))
0009      CCC(K,L,M) = .5*(CC(K,L-M) + CC(K,L+M))
0010      F(I,J) = CC(I,J)
0011      FF(N,L) = F(N-1,L-1) - F(N-1,L+1) - F(N+1,L-1) + F(N+1,L+1)
0012      PFF(K,M) = -FLCAT(M-1)**2*(F(M-1,K-1) - F(M-1,K+1))
1      + FLOAT(M+1)**2*(F(M+1,K-1) - F(M+1,K+1))
0013      PFFF(K,M) = FLOAT(M-1)**4*(F(M-1,K-1) - F(M-1,K+1)) -
1      FLOAT(M+1)**4*(F(M+1,K-1) - F(M+1,K+1))
0014      GCCA(L,I,J) = .5*(FLOAT((I-1)*(J-1))*(F(I-J,L-1)
1      - F(I-J,L+1) - F(I+J-2,L-1) + F(I+J-2,L+1))
2      - FLOAT((I-1)*(J+1))*(F(I-J-2,L-1) - F(I-J-2,L+1)
3      - F(I+J,L-1) + F(I+J,L+1)) - FLOAT((I+1)*(J-1))*(F(I-J+2,L-1)
4      - F(I-J+2,L+1) - F(I+J,L-1) + F(I+J,L+1)) + FLOAT((I+1)*(J+1))
5      *(F(I-J,L-1) - F(I-J,L+1) - F(I+J+2,L-1) + F(I+J+2,L+1)))
0015      GCCB(L,J,I) = -.5*(FLOAT(I-1)**2*(F(I+J-2,L-1) - F(I+J-2,L+1)
1      + F(I-J,L-1) - F(I-J,L+1) - F(I+J,L-1) + F(I+J,L+1)
2      - F(I-J-2,L-1) + F(I-J-2,L+1)) - FLOAT(I+1)**2*
3      (F(I+J,L-1) - F(I+J,L+1) + F(I-J+2,L-1) - F(I-J+2,L+1)
4      - F(I+J+2,L-1) + F(I+J+2,L+1) - F(I-J,L-1) + F(I-J,L+1)))
0016      PI = 3.14159
0017      PI2 = PI*PI
0018      PI3 = PI2*PI
0019      PI4 = PI3*PI
0020      READ(5,110) AB,NU
0021      110      FORMAT(4E10.3)
0022      WRITE(6,1101) AB,NU
0023      1101      FORMAT(1H0,1P4E10.3)
0024      WRITE(6,1)
0025      READ(5,120) NV
0026      WRITE(6,120) NV
0027      120      FORMAT(I5)
0028      WRITE(6,1)
0029      1      FORMAT(1H0)
0030      2      FORMAT(1H1)
0031      AB2 = AB**2
0032      AB4 = AB**4
C      COMPUTE B
0033      NX = 2*NV+2
0034      NY = 3
0035      DO 10 K = 1,NX
0036      DO 10 I = 1,NY
0037      L = 2*I - 1
0038      DO 10 M = 1,NX
0039      DO 10 J = 1,NY

```

```

0040      N = 2*J - 1
0041      AA(K,I,M,J) = FFFF(K,M)*FF(L,N) + 2.*AB2*FFF(K,M)*FFF(L,N)
          1 + AB4*FF(K,M)*FFFF(L,N)
0042      10      CONTINUE
          C      INVPRT AA AND STORE IN AA
0043      NAM = NX*NY
0044      I = 0
0045      J = 0
0046      DO 512 K = 1,NX
0047      DO 512 L = 1,NY
0048      I = I+1
0049      DO 508 M = 1,NX
0050      DO 508 N = 1,NY
0051      J = J+1
0052      508      AM(I,J) = AA(K,L,M,N)
0053      512      J = 0
0054      CALL MATIN2(AM,NA1,90,AMW,90,AVW,KINV,180)
0055      WRITE (6,1)
0056      WRITE (6,511) KINV
0057      511      FORMAT (I10)
0058      I = 0
0059      J = 0
0060      DO 522 K = 1,NX
0061      DO 522 L = 1,NY
0062      I = I+1
0063      DO 518 M = 1,NX
0064      DO 518 N = 1,NY
0065      J = J+1
0066      518      AA(K,L,M,N) = AM(I,J)
0067      522      J = 0
0068      DO 14 I = 1,NV
0069      DO 14 K = 1,NX
0070      DO 14 J = 1,NY
0071      L = 2*J - 1
0072      DO 14 M = 1,NV
0073      V(I,K,J,M) = AB2*(GCCB(I,K,M)*GCCB(1,1,L) - 2.*GCCA(I,K,M)
          1 *GCCA(1,L,1) + GCCB(I,M,K)*GCCB(1,L,1))*PI4
0074      14      CONTINUE
0075      DO 16 K = 1,NX
0076      DO 16 J = 1,NY
0077      L = 2*J - 1
0078      DO 16 M = 1,NV
0079      DO 16 N = 1,NV
0080      G(K,J,M,N) = 12.*(1. - NU**2)*AB2*(GCCA(K,M,N)*GCCA(L,1,1)
          1 - GCCB(K,N,M)*GCCB(L,1,1))
0081      16      CONTINUE
0082      DO 22 I = 1,NV
0083      DO 22 L = I,NV
0084      IVSUM = I+L
0085      DO 22 J = 1,NV
0086      DO 22 K = 1,NV
0087      IGSUM = J+K
0088      B(I,J,K,L) = 0.
0089      IS = I+J+K+L
0090      M = IS-2*(IS/2)
0091      IF(M.NE.0) GO TO 21

```

```
0092      IVS = IVSUM-2*(IVSUM/2)+1
0093      DO 18 IM = IVS,NX,2
0094      IGS = IGSUM-2*(IGSUM/2)+1
0095      DO 18 KK = IGS,NX,2
0096      DO 18 JJ = 1,NY
0097      DO 18 LL = 1,NY
0098      18      B(I,J,K,L) = B(I,J,K,L) + V(I,IM,JJ,L)*AA(IM,JJ,KK,LL)
0099      1      *G(KK,LL,J,K)
0100      21      B(I,J,K,L) = -B(I,J,K,L)
0101      21      CONTINUE
0102      22      B(L,J,K,I) = B(I,J,K,L)
0103      22      CONTINUE
0104      C      WRITE NONLINEAR TERMS ONTO TAPE
0105      WRITE(10) B
0106      ENDFILE 10
0107      WRITE (6,2)
0108      DO 45 I = 1,NV
0109      DO 45 J = 1,NV
0110      DO 45 K = 1,NV
0111      45      WRITE (6,47) (B(I,J,K,L), L = 1,NV)
0112      47      FORMAT(10E12.4)
0113      STOP
0114      END
```

```
0001      FUNCTION CC(K,M)
0002      CC = 0.
0003      IF(K.EQ.M) CC = CC+.5
0004      IF(K.EQ.-M) CC = CC+.5
0005      RETURN
0006      END
```

```

0001      SUBROUTINE MATIN2(A,N1,IA,X,IX,B,INT,N2)
C        THIS SUBROUTINE INVERTS THE UPPER LEFT N1 BY N1 CORNER OF
C        MATRIX A, WHICH WHICH HAS AN ACTUAL FIRST DIMENSION OF IA.
C        X AND B ARE DOUBLE PRECISION MATRICES NEEDED FOR WORKING
C        SPACE-X MUST BE A DOUBLY DIMENSIONED MATRIX WITH FIRST
C        DIMENSION IX, B IS SINGLY DIMENSIONED AND SHOULD BE OF
C        LENGTH AT LEAST 2*N1. INT IS AN INTEGER VARIABLE WHICH
C        IS RETURNED EQUAL TO TWO IF THE MATRIX IS TOO ILL
C        CONDITIONED TO BE INVERTED
C        MODIFIED JORDAN ELIMINATION
0002      DOUBLE PRECISION B(N2),X(IX,N1),PIVOT,TEMP,DABS
0003      DIMENSION A(IA,N1)
0004      INT=1
0005      N=N1
0006      DO 15 I=1,N
0007      DO 15 J=1,N
0008      15  X(I,J)=A(I,J)
0009      DO 9 K=1,N
C        FIND THE PIVOT
0010      PIVOT=0.
0011      DO 1 I=K,N
0012      DO 1 J=K,N
0013      IF(DABS(X(I,J)).LE.DABS(PIVOT)) GO TO 1
0014      PIVOT=X(I,J)
0015      A(1,K)=I
0016      A(2,K)=J
0017      1  CONTINUE
0018      IF(K.EQ.1) COMP=DABS(PIVOT)
0019      IF((K.EQ.1.AND.COMP.LE.1.E-30).OR.
1 DABS(PIVOT).LE.1.E-09*COMP) GO TO 14
C        EXCHANGE ROWS
0020      L=A(1,K)+1.E-6
0021      IF(L.EQ.K) GO TO 3
0022      DO 2 J=1,N
0023      TEMP=X(L,J)
0024      X(L,J)=X(K,J)
0025      2  X(K,J)=TEMP
C        EXCHANGE COLUMNS
0026      3  L=A(2,K)+1.E-6
0027      IF(L.EQ.K) GO TO 5
0028      DO 4 I=1,N
0029      TEMP=X(I,L)
0030      X(I,L)=X(I,K)
0031      4  X(I,K)=TEMP
C        JORDAN STEP
0032      5  DO 8 J=1,N
0033      J2=N+J
0034      B(J)=1.DO/PIVOT
0035      IF(J.NE.K) GO TO 6
0036      B(J2)=1.DO
0037      GO TO 7
0038      6  B(J)=-X(K,J)*B(J)
0039      B(J2)=X(J,K)
0040      7  X(K,J)=0.
0041      8  X(J,K)=0.
0042      DO 9 I=1,N

```

```
0043      I2=N+I
0044      DO 9 J=1,N
0045      9 X(I,J)=X(I,J)+B(I2)*B(J)
      C REORDER FINAL MATRIX
0046      DO 13 L=1,N
0047      K=N+1-L
0048      J=A(1,K)+1.E-6
0049      IF(J.EQ.K) GO TO 11
0050      DO 10 I=1,N
0051      TEMP=X(I,J)
0052      X(I,J)=X(I,K)
0053      10 X(I,K)=TEMP
0054      11 I=A(2,K)+1.E-6
0055      IF(I.EQ.K) GO TO 13
0056      DO 12 J=1,N
0057      TEMP=X(I,J)
0058      X(I,J)=X(K,J)
0059      12 X(K,J)=TEMP
0060      13 CONTINUE
0061      DO 25 I=1,N
0062      DO 25 J=1,N
0063      25 A(I,J)=X(I,J)
0064      RETURN
0065      14 INT=2
0066      RETURN
0067      END
```

COMPILER OPTIONS - NAME= MAIN,OPT=02,LINECNT=58,SIZE=0000K,
SOURCE,EBCDIC,NOLIST,NODECK,LOAD,MAP,NOEDIT,ID,NOXREF

```

C      PROGRAM TO COMPUTE AERODYNAMIC ADMITTANCE FUNCTIONS
C      FOR PLATES WITH CLAMPED EDGES
C      EM IS MACH NUMBER
C      DO NOT USE EM = 1.0
C      AB IS PLATE LENGTH/WIDTH RATIO
C      MMAX IS THE NUMBER OF MODES USED IN THE EXPRESSION
C      FOR THE PLATE DEFLECTION
C      IMAX IS THE NUMBER OF POINTS AT WHICH EACH
C      ADMITTANCE FUNCTION IS TO BE COMPUTED
C      THE AEH'S AND AEI'S ARE THE ADMITTANCE FUNCTIONS
ISN 0002      DIMENSION AEH(12,12,100),AEI(12,12,100)
ISN 0003      DIMENSION PERM(5000)
ISN 0004      READ(5,11) EM,AB,MMAX,IMAX
ISN 0005      WRITE(6,11) EM,AB,MMAX,IMAX
ISN 0006      11      FORMAT (2F10.4, 2I10)
ISN 0007      DO 1011 I= 1,MMAX
ISN 0008      DO 1011 J= 1,MMAX
ISN 0009      DO 1011 K= 1,100
ISN 0010      AEH(I,J,K)= 0.
ISN 0011      1011 AEI(I,J,K)= 0.
ISN 0012      CIMAX=IMAX
ISN 0013      CMMAX=MMAX
ISN 0014      PI = 3.14159
ISN 0015      SIGF = EM/(EM-1.)
ISN 0016      IF(EM.GT.1.) GO TO 15
ISN 0018      EMP = EM**2/(1.-EM**2)
ISN 0019      ABP = (AB**2+1.)/AB**2
ISN 0020      SIGF = EMP + SQRT(EMP**2+EMP*ABP)
ISN 0021      15      CONTINUE
ISN 0022      DELSIG = SIGF/CIMAX
ISN 0023      WRITE (6,17) SI;F, DELSIG
ISN 0024      17      FORMAT(2E20.4)
ISN 0025      GAMMAX=3.*PI
ISN 0026      ALPMAX=SQRT((PI*(CMMAX+1.))**2+100.)+5.
ISN 0027      DO 24 I=1,IMAX
ISN 0028      CI=I
ISN 0029      S=CI*DELSIG
ISN 0030      DELGAM=PI/4.
ISN 0031      DELALP=PI/(4.*(1.+2*S*(EM+1.)/EM))
ISN 0032      DEL = -DELGAM*DELALP/(PI*EM)**2
ISN 0033      NGAM=GAMMAX/DELGAM
ISN 0034      NALP=ALPMAX/DELALP
ISN 0035      WRITE(6,99) NALP,NGAM
ISN 0036      99      FORMAT(2I20)
ISN 0037      X= DELALP/2.
ISN 0038      DO 22 L=1,NALP
ISN 0039      GERM=0.
ISN 0040      GAM=.01
ISN 0041      DO 23 K=1,NGAM
ISN 0042      SQ=SQRT(X**2+GAM**2*AB**2)
ISN 0043      Z=SQ*S/EM
ISN 0044      CALL GMR(GAM,1,1,GR,GI)
ISN 0045      45      C=GR
ISN 0046      GERM=GERM+C*SQ*BJ1(Z)

```



```

ISN 0047      23      GAM=GAM+DELGAM
ISN 0048      FERM(L)=G3RM
ISN 0049      22      X=X+DELALP
ISN 0050      DO 21 M=1,MMAX
ISN 0051      DO 21 MR=M,MMAX
ISN 0052      ALPH= DELALP/2.
ISN 0053      TERMH=0.
ISN 0054      TERMI=0.
ISN 0055      DO 10 J=1,NALP
ISN 0056      CALL GMR(ALPH,M,MR,GR,GI)
ISN 0057      TERMH=TERMH+(GR*SIN (ALPH*S)-GI*COS (ALPH*S))
1 *FERM(J)*ALPH
ISN 0058      TERMI=TERMI+(GR*COS (ALPH*S)+GI*SIN (ALPH*S))*FERM(J)
ISN 0059      10      ALPH=ALPH+DELALP
ISN 0060      AEH(M,MR,I)=TERMH*DEL
ISN 0061      AEI(M,MR,I)=TERMI*DEL
ISN 0062      WRITE(6,12) AEH(M,MR,I),AEI(M,MR,I),M,MR,I
ISN 0063      12      FORMAT (2E20.3,3I10)
ISN 0064      21      CONTINUE
ISN 0065      24      CONTINUE
ISN 0066      199     FORMAT(6E20.3)
C      WRITE ADMITTANCE FUNCTIONS ONTO TAPE
ISN 0067      WRITE (10) AEH,AEI,EM,AB,SIGP,IMAX
ISN 0068      ENDFILE 10
ISN 0069      STOP
ISN 0070      END

```

COMPILER OPTIONS - NAME= MAIN,OPT=02,LINECNT=58,SIZE=0000K,
SOURCE,EBCDIC,NOLIST,NODECK,LOAD,MAP,NOEDIT,ID,NOXREF

```

ISN 0002      SUBROUTINE GMR(X,M,N,GR,GI)
                C      CLAMPED PLATE
ISN 0003      XX = X
ISN 0004      PI = 3.14159
ISN 0005      AM = M
ISN 0006      AN = N
ISN 0007      A = PI*(AM-1.)
ISN 0008      B = PI*(AM+1.)
ISN 0009      C = PI*(AN-1.)
ISN 0010      D = PI*(AN+1.)
ISN 0011      14  CONTINUE
ISN 0012      DENOM = (X**2-A**2)*(X**2-B**2)*(X**2-C**2)
                1 *(X**2-D**2)
ISN 0013      IF (ABS(DENOM).LT.1.0E-10) GO TO 12
ISN 0015      GR = AMP*((1.+(-1.)**(M+N))*((-1.)**M+(-1.)**N)
                1 *COS(X))
ISN 0016      GI = AMP*SIN (X)*((-1.)**N - (-1.)**M)
ISN 0017      X = XX
ISN 0018      RETURN
ISN 0019      12  CONTINUE
ISN 0020      X = X+.01
ISN 0021      GO TO 14
ISN 0022      END

```

COMPILER OPTIONS - NAME= MAIN,OPT=02,LINECNT=58,SIZE=0000K,
SOURCE,BCDIC,NOLIST,NODECK,LOAD,HAP,NOEDIT,ID,NOXREF

```
ISN 0002      FUNCTION BJ1(X)
                C      POLYNOMIAL APPROXIMATION FOR BESSEL FUNCTION
ISN 0003      IF (X-3.) 1,2,2
ISN 0004      1      Y=(X/3.)*2
ISN 0005      BJ1=X*(.5-.56249985*Y+.21093573*Y**2-.03954289*Y**3+
                1      .00443319*Y**4-.00031761*Y**5+.00001109*Y**6)
ISN 0006      GO TO 3
ISN 0007      2      Y=3./X
ISN 0008      F1=.79788456+.00000156*Y+.01659667*Y**2+.00017105*Y**3-
                1      .00249511*Y**4+.00113653*Y**5-.00020033*Y**6
ISN 0009      TH1=X-2.35619449+.12499612*Y+.00005656*Y**2-.00637879*Y**3+
                1      .00074348*Y**4+.00079824*Y**5-.00029166*Y**6
ISN 0010      BJ1=F1*COS (TH1)/SQRT (X)
ISN 0011      3      CONTINUE
ISN 0012      RETURN
ISN 0013      END
```

COMPILER OPTIONS - NAME= MAIN,OPT=02,LINECNT=58,SIZE=0000K,
SOURCE,EBCDIC,NOLIST,NODECK,LOAD,MAP,NOEDIT,ID,NOXREF

C FLUTTER PROGRAM FOR CLAMPED-EDGE PLATES USING
C LINEARIZED POTENTIAL FLOW AERODYNAMICS
C LAMDA=DYNAMIC PRESSURE,NU=FLOW DENSITY,MACH=MACH NUMBER
C AB=PLATE LENGTH/WIDTH RATIO,RXA,RYA=APPLIED IN-PLANE
C LOAD (POSITIVE IN TENSION),PSTAT=STATIC PRESSURE
C DIFFERENTIAL, CAVITY=CAVITY ACOUSTIC PARAMETER
C DAMP=STRUCTURAL DAMPING FACTOR
C NV=#OF MODES,H=INTEGRATION STEP INTERVAL,TPRINT=PRINT-OUT
C INTERVAL,TFINAL=TIME AT WHICH INTEGRATION STOPS
C SCALE=MAXIMUM ANTICIPATED DEFLECTION (FOR GRAPH ROUTINE)
C X, .. = ALPHANUMERIC CHARACTERS FOR GRAPH ROUTINE
C THE A'S ARE MODAL AMPLITUDES
C THE W'S ARE THE PANEL DEFLECTION AT 15 EVENLY SPACED POINTS
C ALONG THE PANEL CENTERLINE
C
C
C
C

REMOVE CARDS #177 THROUGH 189 FOR ZERO EDGE RESTRAINT
CALCULATION
C
C
C

ISN 0002 REAL LAMDA, MU
ISN 0003 REAL NU
ISN 0004 REAL MACH
ISN 0005 DIMENSION B(12,12,12,12)
ISN 0006 DIMENSION ABH(12,12,100),AEI(12,12,100)
ISN 0007 DIMENSION AS(500,12),DAS(500,12)
ISN 0008 DIMENSION S(12,12),C(12,12),D(12,12),PHIX(12,12),PHIY(12,12)
ISN 0009 DIMENSION A(12),DA(12),DDA(12),DDAS(4,12)
ISN 0010 DIMENSION Q(12,12)
ISN 0011 DIMENSION W(15),F(12)
ISN 0012 DIMENSION ST(12,12)
ISN 0013 DIMENSION WM(12,12)
ISN 0014 DIMENSION WV(24)
ISN 0015 DIMENSION RINE(61)
ISN 0016 REAL*8 WM
ISN 0017 REAL*8 WV
ISN 0018 PP(I,M) = CC(I-1,M-1)-CC(I-1,M+1)-CC(I+1,M-1)+CC(I+1,M+1)
ISN 0019 PPX(I,J) = -PI*FLOAT(J-1)*(CS(I-1,J-1)-CS(I+1,J-1))
1 + PI*FLOAT(J+1)*(CS(I-1,J+1)-CS(I+1,J+1))
ISN 0020 PPXX(I,M) = -PI2*FLOAT(M-1)**2*(CC(I-1,M-1)-CC(I+1,M-1))
1 + PI2*FLOAT(M+1)**2*(CC(I-1,M+1)-CC(I+1,M+1))
ISN 0021 PPXXX(I,M) = PI4*FLOAT(M-1)**4*(CC(I-1,M-1)-CC(I+1,M-1))
1 - PI4*FLOAT(M+1)**4*(CC(I-1,M+1)-CC(I+1,M+1))
ISN 0022 1 FORMAT (1H0)
ISN 0023 2 FORMAT (1H1)
ISN 0024 PI = 3.14159
ISN 0025 PI2 = PI*PI
ISN 0026 PI3 = PI2*PI
ISN 0027 PI4 = PI3*PI
ISN 0028 NU = .3
ISN 0029 READ (5,701) CROSS, BLANK, DOT, SCALE
ISN 0030 701 FORMAT (3A1, F7.1)
ISN 0031 WRITE (6,700) CROSS, BLANK, DOT, SCALE
ISN 0032 700 FORMAT (1X, 3A1, F7.2)

```

ISN 0033          SCALE = 30./SCALE
ISN 0034          DO 702 I = 1,61
ISN 0035          702  RINE(I) = BLANK
                   C    READ NONLINEAR TERMS FROM TAPE
ISN 0036          READ(10) B
ISN 0037          REWIND 10
                   C    READ AERODYNAMIC ADMITTANCE FUNCTIONS FROM TAPE
ISN 0038          READ(12) AEH,AEI,MACH,AB,SIGF,ISMAX
ISN 0039          REWIND 12
ISN 0040          WRITE (6,1)
ISN 0041          WRITE (6,13) MACH,AB,NV,ISMAX,SIGF
ISN 0042          13  FORMAT(2F10.4,2I10,E10.3)
ISN 0043          5   FORMAT (1P8E9.2)
ISN 0044          8   FORMAT (10E12.3)
ISN 0045          WRITE (6,1)
ISN 0046          READ (5,110) LAMDA, MU, PSTAT, CAVITY
ISN 0047          110 FORMAT(4E10.3)
ISN 0048          WRITE(6,1101) LAMDA,MU,PSTAT,CAVITY
ISN 0049          1101 FORMAT(1H0,1P4E10.3)
ISN 0050          READ (5,110) RXA,RYA
ISN 0051          WRITE(6,1101) RXA,RYA
ISN 0052          WRITE (6,1)
ISN 0053          READ (5,116) DAMP
ISN 0054          116 FORMAT(E10.3)
ISN 0055          WRITE (6,117) DAMP
ISN 0056          117 FORMAT(' STRUCTURAL DAMPING= ',E12.3)
ISN 0057          WRITE (6,1)
ISN 0058          READ (5,1113) NV,H,TPRINT,TFINAL
ISN 0059          WRITE (6,1113) NV,H,TPRINT,TFINAL
ISN 0060          1113 FORMAT (I10,3E10.3)
ISN 0061          WRITE (6,1)
ISN 0062          READ (5,113) (A(I), I = 1,NV)
ISN 0063          WRITE (6,115) (A(I), I = 1,NV)
ISN 0064          READ (5,113) (DA(I), I = 1,NV)
ISN 0065          WRITE (6,115) (DA(I), I = 1,NV)
ISN 0066          113 FORMAT(6E10.3)
ISN 0067          115 FORMAT(1X,6E12.3)
ISN 0068          AB2 = AB**2
ISN 0069          AB4 = AB**4
ISN 0070          RISMAX = ISMAX
ISN 0071          DELS = SIGF/RISMAX
ISN 0072          ROOT = SQRT(LAMDA/MU)
ISN 0073          HAERO = ROOT*H
ISN 0074          NAERO = DELS/HAERO
ISN 0075          IF(NAERO.LT.1) GO TO 404
ISN 0077          IF(NAERO.GT.20) NAERO = 20
ISN 0079          DELSIG = NAERO*HAERO
ISN 0080          IMAX = SIGF/DELSIG
ISN 0081          GO TO 406
ISN 0082          404 CONTINUE
ISN 0083          NAERO = 1
ISN 0084          DELSIG = DELS
ISN 0085          H = DELSIG/ROOT
ISN 0086          IMAX = ISMAX
ISN 0087          406 CONTINUE
ISN 0088          HP = DELSIG/ROOT

```

```

ISN 0089      WRITE (6,1)
ISN 0090      WRITE(6,401) H,DELSIG,NAERO,IMAX
ISN 0091      401  FORMAT(2E20.3,2I5)
ISN 0092      IF(IMAX.GT.100) STOP
ISN 0094      NSTORE = NAERO*IMAX
ISN 0095      DO 3 I= 1,NV
ISN 0096      DO 3 J= 1,NV
ISN 0097      DO 3 K= 1,ISMAX
ISN 0098      AEH(I,J,100-K+1) = AEH(I,J,ISMAX-K+1)
ISN 0099      AEI(I,J,100-K+1) = AEI(I,J,ISMAX-K+1)
ISN 0100      3  CONTINUE
ISN 0101      IP = 100-ISMAX+1
ISN 0102      DO 400 M = 1,NV
ISN 0103      DO 400 N = M,NV
ISN 0104      DO 400 I = 1,IMAX
ISN 0105      X = FLOAT(I)*DELSIG/DELS
ISN 0106      J = INT(X)
ISN 0107      P=X-AINT(X)
ISN 0108      JP=IP-1+J
ISN 0109      IF (J) 300,300,301
ISN 0110      300  AEH(M,N,I)=AEH(1,N,JP+1)*P
ISN 0111      AEI(M,N,I)=AEI(1,N,JP+1)*P
ISN 0112      GO TO 400
ISN 0113      301  AEH(M,N,I) = AEH(M,N,JP)*(1.-P) + AEH(M,N,JP+1)*P
ISN 0114      AEI(M,N,I) = AEI(M,N,JP)*(1.-P) + AEI(M,N,JP+1)*P
ISN 0115      400  CONTINUE
ISN 0116      DO 410 M = 1,NV
ISN 0117      DO 410 N = M,NV
ISN 0118      DO 410 I = 1,IMAX
ISN 0119      AEH(N,M,I) = (-1.)**(M+N)*AEH(M,N,I)
ISN 0120      AEI(N,M,I) = (-1.)**(M+N)*AEI(M,N,I)
ISN 0121      410  CONTINUE
ISN 0122      DO 30 I = 1,NV
ISN 0123      DO 30 J = 1,NV
ISN 0124      S(I,J) = PP(I,J)*PP(1,1)
ISN 0125      ST(I,J) = S(I,J)
ISN 0126      C(I,J) = PPXXX(I,J)*PP(1,1) + 2.*AB2*PPXX(I,J)*PPXX(1,1)
ISN 0127      1  + AB4*PP(I,J)*PPXXX(1,1)
ISN 0128      D(I,J) = PPX(I,J)*PP(1,1)
ISN 0129      PHIX(I,J) = -PPXX(I,J)*PP(1,1)
ISN 0130      PHIY(I,J) = -PP(I,J)*PPXX(1,1)
ISN 0131      30  CONTINUE
ISN 0132      WRITE(6,1)
ISN 0133      DO 910 I = 1,NV
ISN 0134      910  WRITE(6,573) ( S(I,J), J = 1,NV)
ISN 0135      WRITE (6,1)
ISN 0136      DO 580 I = 1,NV
ISN 0137      580  WRITE (6,573) (C(I,J), J = 1,NV)
ISN 0138      573  FORMAT (8E16.4)
ISN 0139      C  INVERT S AND STORE IN S
ISN 0140      CALL MATIN2(S,NV,12,MM,12,WV,KINVRT,24)
ISN 0141      WRITE(6,1)
ISN 0142      5067 WRITE(6,5067) KINVRT
ISN 0143      FORMAT(I5)
ISN 0144      WRITE(6,1)
ISN 0145      DO 912 I = 1,NV

```

```

ISN 0144      912      WRITE(6,573) ( D(I,J) , J = 1,NV)
ISN 0145      WRITE(6,1)
ISN 0146      DO 914 I = 1,NV
ISN 0147      914      WRITE(6,573) (PHIX(I,J) , J = 1,NV)
ISN 0148      WRITE(6,1)
ISN 0149      DO 916 I = 1,NV
ISN 0150      916      WRITE(6,573) (PHIY(I,J) , J = 1,NV)
ISN 0151      WRITE (6,1)
C              SET UP INTEGRATION
ISN 0152      T = 0.
ISN 0153      TP = 0.
ISN 0154      DO 70 I = 1,500
ISN 0155      DO 70 J = 1,NV
ISN 0156      AS(I,J) = 0.
ISN 0157      70      DAS(I,J) = 0.
ISN 0158      DO 74 I = 1,4
ISN 0159      DO 74 J = 1,NV
ISN 0160      74      DDAS(I,J) = 0.
ISN 0161      IMAXP = IMAX - 1
ISN 0162      HHH = H/24.
ISN 0163      WRITE (6,2)
C              PREDICTOR ROUTINE
ISN 0164      56      CONTINUE
ISN 0165      IF(A(1).GT.10.) STOP
C              COMPUTE SECOND DIRIVATIVES
ISN 0167      DO 490 I = 1,NV
ISN 0168      DO 490 J = 1,NV
ISN 0169      Q(I,J) = (D(I,J)*A(J) + ST(I,J)*DA(J)/ROOT)/MACH
ISN 0170      DO 488 K = 1,IMAXP
ISN 0171      KP = NAERO*K
ISN 0172      Q(I,J) = Q(I,J)+DAS(KP,J)*AEI(J,I,K)*HP
1      *AS(KP,J)*AEH(J,I,K)*DELSIG
ISN 0173      488      CONTINUE
ISN 0174      490      CONTINUE
ISN 0175      SX = 0.
ISN 0176      SY = 0.
C              REMOVE THE FOLLOWING 12 CARDS FOR A ZERO EDGE RESTRAINT
C              CALCULATION
ISN 0177      SY = .5*A(1)**2
ISN 0178      DO 212 M = 1,NV
ISN 0179      RM = M
ISN 0180      SX = SX + (RM**2+1.)*A(M)**2
ISN 0181      212      SY = SY + A(M)**2
ISN 0182      NVP = NV-2
ISN 0183      IF(NVP.LT.1) GO TO 215
ISN 0185      DO 214 M = 1,NVP
ISN 0186      RM = M
ISN 0187      SX = SX - (RM+1.)**2*A(M)*A(M+2)
ISN 0188      214      SY = SY - A(M)*A(M+2)
ISN 0189      215      CONTINUE
ISN 0190      AB2RXB = 12.*PI2*(.75*SX + NU*AB2*SY) + RXA
ISN 0191      RYB = 12.*PI2*(AB2*SY + NU*.75*SX) + RYA
ISN 0192      DO 250 I = 1,NV
ISN 0193      F(I) = 0.
ISN 0194      DO 216 M = 1,NV
ISN 0195      216      F(I) = F(I) - AB2RXB*PHIX(I,M)*A(M) - AB2*RYB*PHIY(I,M)*A(M)

```

```

ISN 0196      DO 220 J = 1,NV
ISN 0197      DO 220 K = 1,NV
ISN 0198      LSUM = I+J+K
ISN 0199      LS = 2*(LSUM/2)-LSUM+2
ISN 0200      DO 220 L = LS,NV,2
ISN 0201      220  F(I) = F(I) - B(I,J,K,L)*A(J)*A(K)*A(L)
ISN 0202      DO 230 J = 1,NV
ISN 0203      230  F(I) = F(I) - C(I,J)*A(J) - LAMDA*Q(I,J)-DAMP*C(I,J)*DA(J)
ISN 0204      250  CONTINUE
ISN 0205      F(1) = F(1) - CAVITY*A(1) + PSTAT
ISN 0206      DO 240 I = 1,NV
ISN 0207      DDA(I) = 0.
ISN 0208      DO 240 J = 1,NV
ISN 0209      DDA(I) = DDA(I) + S(I,J)*F(J)
ISN 0210      240  CONTINUE
ISN 0211      C      PRINT OUTPUT
ISN 0213      IF(T.LT.TP) GO TO 350
ISN 0213      TP = TP + TPRINT
ISN 0213      C      PRINT MODAL AMPLITUDES, VELOCITIES, AND ACCELERATIONS
ISN 0214      WRITE (6,345) T
ISN 0215      345  FORMAT(6H TIME=,F7.4)
ISN 0216      WRITE (6,347) (A(I), I = 1,NV)
ISN 0217      WRITE (6,347) (DA(I), I = 1,NV)
ISN 0218      WRITE (6,347) (DDA(I), I = 1,NV)
ISN 0219      347  FORMAT(6E11.3)
ISN 0220      DO 348 I = 1,15
ISN 0221      W(I) = 0.
ISN 0222      THETA = PI*FLOAT(I)/16.
ISN 0223      DO 346 J = 1,NV
ISN 0224      346  W(I) = W(I) + 2.*A(J)*(COS (FLOAT(J-1)*THETA) - COS (FLOAT(J+1)
ISN 0224      1 *THETA))
ISN 0225      348  CONTINUE
ISN 0225      C      PRINT PLATE DEFLECTION AT 15 EQUALLY SPACED POINTS ALONG THE
ISN 0225      C      CENTERLINE OF THE PANEL
ISN 0226      WRITE (6,349) (W(I), I = 1,15)
ISN 0227      349  FORMAT (8F7.2)
ISN 0228      RINE(1) = DOT
ISN 0229      RINE(31) = DOT
ISN 0230      RINE(61) = DOT
ISN 0231      L = SCALE*W(12)
ISN 0232      LP = 31+L
ISN 0233      IF (IABS(L).LE.30) RINE(LP) = CROSS
ISN 0233      C      GRAPH DEFLECTION OF POINT ON LATERAL CENTERLINE OF PANEL
ISN 0233      C      3/4 OF WAY BACK FROM LEADING EDGE
ISN 0235      WRITE (6,703) (RINE(I), I = 1,61)
ISN 0236      703  FORMAT (68X, 61A1)
ISN 0237      IF (IABS(L).LE.30) RINE(LP) = BLANK
ISN 0239      IF (T.GE.TFINAL) GO TO 57
ISN 0241      350  CONTINUE
ISN 0241      C      STORE VARIABLES
ISN 0242      DO 24 J = 2,NSTORE
ISN 0243      K = NSTORE-J+2
ISN 0244      KP = K-1
ISN 0245      DO 24 I = 1,NV
ISN 0246      AS(K,I) = AS(KP,I)
ISN 0247      DAS(K,I) = DAS(KP,I)

```


ISN 0248	24	CONTINUE
ISN 0249		DO 26 J = 2,4
ISN 0250		K = 6-J
ISN 0251		KP = K-1
ISN 0252		DO 26 I = 1,NV
ISN 0253		DDAS(K,I) = DDAS(KP,I)
ISN 0254	26	CONTINUE
ISN 0255		DO 28 I = 1,NV
ISN 0256		AS(1,I) = A(I)
ISN 0257		DAS(1,I) = DA(I)
ISN 0258		DDAS(1,I) = DDA(I)
ISN 0259	28	CONTINUE
	C	PREDICT
ISN 0260		DO 20 I = 1,NV
ISN 0261		A(I) = A(I)+HHH*(55.*DAS(1,I)-59.*DAS(2,I)
	1	+37.*DAS(3,I)-9.*DAS(4,I))
ISN 0262		DA(I) = DA(I)+HHH*(55.*DDAS(1,I)-59.*DDAS(2,I)
	1	+37.*DDAS(3,I)-9.*DDAS(4,I))
ISN 0263	20	CONTINUE
ISN 0264		T = T+H
ISN 0265		GO TO 56
ISN 0266	57	CONTINUE
ISN 0267		STOP
ISN 0268		END

COMPILER OPTIONS - NAME= MAIN,OPT=02,LINECNT=58,SIZE=0000K,
SOURCE,EBCDIC,NOLIST,NODECK,LOAD,MAP,NOEDIT,ID,NOXREF

```

ISN 0002      SUBROUTINE MATIN2(A,N1,IA,X,IX,B,INT,N2)
C            THIS SUBROUTINE INVERTS THE UPPER LEFT N1 BY N1 CORNER OF
C            MATRIX A, WHICH WHICH HAS AN ACTUAL FIRST DIMENSION OF IA.
C            X AND B ARE DOUBLE PRECISION MATRICES NEEDED FOR WORKING
C            SPACE-X MUST BE A DOUBLY DIMENSIONED MATRIX WITH FIRST
C            DIMENSION IX, B IS SINGLY DIMENSIONED AND SHOULD BE OF
C            LENGTH AT LEAST 2*N1. INT IS AN INTEGER VARIABLE WHICH
C            IS RETURNED EQUAL TO TWO IF THE MATRIX IS TOO ILL
C            CONDITIONED TO BE INVERTED
C            MODIFIED JORDAN ELIMINATION
ISN 0003      DOUBLE PRECISION B(N2),X(IX,N1),PIVOT,TEMP,DABS
ISN 0004      DIMENSION A(IA,N1)
ISN 0005      INT=1
ISN 0006      N=N1
ISN 0007      DO 15 I=1,N
ISN 0008      DO 15 J=1,N
ISN 0009      15 X(I,J)=A(I,J)
ISN 0010      DO 9 K=1,N
C            FIND THE PIVOT
ISN 0011      PIVOT=0.
ISN 0012      DO 1 I=K,N
ISN 0013      DO 1 J=K,N
ISN 0014      IF(DABS(X(I,J)).LE.DABS(PIVOT)) GO TO 1
ISN 0016      PIVOT=X(I,J)
ISN 0017      A(1,K)=I
ISN 0018      A(2,K)=J
ISN 0019      1 CONTINUE
ISN 0020      IF(K.EQ.1) COMP=DABS(PIVOT)
ISN 0022      IF((K.EQ.1.AND.COMP.LE.1.E-30).OR.
1 DABS(PIVOT).LE.1.5E-09*COMP) GO TO 14
C            EXCHANGE ROWS
ISN 0024      L=A(1,K)+1.E-6
ISN 0025      IF(L.EQ.K) GO TO 3
ISN 0027      DO 2 J=1,N
ISN 0028      TEMP=X(L,J)
ISN 0029      X(L,J)=X(K,J)
ISN 0030      2 X(K,J)=TEMP
C            EXCHANGE COLUMNS
ISN 0031      3 L=A(2,K)+1.E-6
ISN 0032      IF(L.EQ.K) GO TO 5
ISN 0034      DO 4 I=1,N
ISN 0035      TEMP=X(I,L)
ISN 0036      X(I,L)=X(I,K)
ISN 0037      4 X(I,K)=TEMP
C            JORDAN STEP
ISN 0038      5 DO 8 J=1,N
ISN 0039      J2=N+J
ISN 0040      B(J)=1.D0/PIVOT
ISN 0041      IF(J.NE.K) GO TO 6
ISN 0043      B(J2)=1.D0
ISN 0044      GO TO 7
ISN 0045      6 B(J)=-X(K,J)*B(J)
ISN 0046      B(J2)=X(J,K)
ISN 0047      7 X(K,J)=0.

```

ISN 0048	8	X(J,K)=0.
ISN 0049		DO 9 I=1,N
ISN 0050		I2=N+I
ISN 0051		DO 9 J=1,N
ISN 0052	9	X(I,J)=X(I,J)+B(I2)*B(J)
	C	REORDER FINAL MATRIX
ISN 0053		DO 13 L=1,N
ISN 0054		K=N+1-L
ISN 0055		J=A(1,K)+1.E-6
ISN 0056		IF(J.EQ.K) GO TO 11
ISN 0058		DO 10 I=1,N
ISN 0059		TEMP=X(I,J)
ISN 0060		X(I,J)=X(I,K)
ISN 0061	10	X(I,K)=TEMP
ISN 0062	11	I=A(2,K)+1.E-6
ISN 0063		IF(I.EQ.K) GO TO 13
ISN 0065		DO 12 J=1,N
ISN 0066		TEMP=X(I,J)
ISN 0067		X(I,J)=X(K,J)
ISN 0068	12	X(K,J)=TEMP
ISN 0069	13	CONTINUE
ISN 0070		DO 25 I=1,N
ISN 0071		DO 25 J=1,N
ISN 0072	25	A(I,J)=X(I,J)
ISN 0073		RETURN
ISN 0074	14	INT=2
ISN 0075		RETURN
ISN 0076		END

COMPILER OPTIONS - NAME= MAIN,OPT=02,LINECNT=58,SIZE=0000K,
SOURCE,EBCDIC,NOLIST,NODECK,LOAD,MAP,NOEDIT,ID,NOXREF

```
ISN 0002      FUNCTION CS(M,N)
ISN 0003      CS = 0.
ISN 0004      PI = 3.14159
ISN 0005      RM = M
ISN 0006      RN = N
ISN 0007      IF(MOD(M+N,2).NE.0) CS = -2.*RN/(PI*(RM**2-RN**2))
ISN 0009      RETURN
ISN 0010      END
```

COMPILER OPTIONS - NAME= MAIN,OPT=02,LINECNT=58,SIZE=0000K,
SOURCE,EBCDIC,NOLIST,NODECK,LOAD,MAP,NOEDIT,ID,NOXREF

```
ISN 0002      FUNCTION CC(K,M)
ISN 0003      CC = 0.
ISN 0004      IF(K.EQ.M) CC = CC+.5
ISN 0006      IF(K.EQ.-M) CC = CC+.5
ISN 0008      RETURN
ISN 0009      END
```

COMPILER OPTIONS - NAME= MAIN,OPT=02,LINECNT=58,SIZE=0000K,
SOURCE,EBCDIC,NOLIST,NODECK,LOAD,MAP,NORDIT,ID,NOXREF

```

C      PROGRAM TO COMPUTE STRESSES DUE TO PLATE DEFLECTION FOR
C      CLAMPED PLATE WITH COMPLETE IN-PLANE EDGE RESTRAINT
C      AB=PLATE LENGTH/WIDTH RATIO,NV=# OF MODES,NU=POISSON'S RATIO
C      XA,YB=COORDINATES OF POINT AT STRESSES ARE COMPUTED
C      (XA,YB ARE NONDIMENSIONALIZED BY PANEL LENGTH & WIDTH)
C      XA=N/16,N=0,1,2,...17
C      YB IS SPECIFIED AS INPUT DATA
C      THE A'S ARE THE MODAL AMPLITUDES (WHICH DEFINE THE PLATE
C      DEFLECTION)
ISN 0002      REAL NU
ISN 0003      DIMENSION A(12)
ISN 0004      DENOM1(K) = (FLOAT(K**2) + 16.*AB2)**2
ISN 0005      DENOM2(K) = (FLOAT(K**2) + 4.*AB2)**2
ISN 0006      B1(M,N) = -FLOAT(2*M*(M+N) + 4)/DENOM1(M-N)
ISN 0007      B2(M,N) = FLOAT((M-1)*(M+N))/DENOM1(M-N-2)
ISN 0008      B3(M,N) = FLOAT((M+1)*(M+N))/DENOM1(M-N+2)
ISN 0009      B4(M,N) = FLOAT(2*M*(M-N) + 4)/DENOM1(M+N)
ISN 0010      B5(M,N) = -FLOAT((M-1)*(M-N))/DENOM1(M+N-2)
ISN 0011      B6(M,N) = -FLOAT((M+1)*(M-N))/DENOM1(M+N+2)
ISN 0012      B7(M,N) = FLOAT(4*M**2 + 4)/DENOM2(M-N)
ISN 0013      B8(M,N) = -FLOAT(2*(M-1)**2)/DENOM2(M-N-2)
ISN 0014      B9(M,N) = -FLOAT(2*(M+1)**2)/DENOM2(M-N+2)
ISN 0015      B10(M,N) = -FLOAT(4*M**2 + 4)/DENOM2(M+N)
ISN 0016      B11(M,N) = FLOAT(2*(M-1)**2)/DENOM2(M+N-2)
ISN 0017      B12(M,N) = FLOAT(2*(M+1)**2)/DENOM2(M+N+2)
ISN 0018      CS(M,X) = COS(FLOAT(M)*PI*X)
ISN 0019      READ (5,697) AB, NV
ISN 0020      WRITE (6,697) AB, NV
ISN 0021      697      FORMAT (F10.3, I10)
ISN 0022      READ (5,697) YB
ISN 0023      WRITE (6,697) YB
ISN 0024      READ (5,699) (A(I), I = 1,NV)
ISN 0025      WRITE (6,699) (A(I), I = 1,NV)
ISN 0026      699      FORMAT (6F10.4)
ISN 0027      PI = 3.14159
ISN 0028      PI2 = PI**2
ISN 0029      PI4 = PI**4
ISN 0030      AB2 = AB**2
ISN 0031      AB4 = AB**4
ISN 0032      NU = .3
ISN 0033      XA = 0.
ISN 0034      CHI = 1. - CS(2,YB)
ISN 0035      DO 710 II = 1,17
ISN 0036      WRITE (6,1)
ISN 0037      1      FORMAT (1H0)
ISN 0038      WRITE (6,701) XA, YB
ISN 0039      701      FORMAT (2320.3)
ISN 0040      W = 0.
ISN 0041      WXX = 0.
ISN 0042      WYY = 0.
ISN 0043      DO 704 M = 1,NV
ISN 0044      PSI = CS(M-1,XA) - CS(M+1,XA)
ISN 0045      RM = M
ISN 0046      PSIXX = -(RM-1.)**2*PI2*CS(M-1,XA) + (RM+1.)**2*PI2*

```

```

1 CS(M+1,XA)
ISN 0047 W = W + A(M)*PSI
ISN 0048 WXX = WXX + PSI*XX*A(M)
ISN 0049 704 WYY = WYY + PSI*A(M)
ISN 0050 W = W*CHI
ISN 0051 WXX = WXX*CHI
ISN 0052 WYY = 4.*PI2*CS(2,YB)*WYY
ISN 0053 WRITE (6,701) W
ISN 0054 WRITE (6,701) WXX, WYY
ISN 0055 SIGMAX = -.5*(WXX + NU*AB2*WYY)
ISN 0056 SIGMAY = -.5*(AB2*WYY + NU*WXX)
C PRINT PLATE BENDING STRESSES AT POINT (XA,YB)
WRITE (6,701) SIGMAX, SIGMAY
ISN 0057 SX = 0.
ISN 0058 SY = .5*A(1)**2
ISN 0059 DO 706 M = 1,NV
ISN 0060 RM = M
ISN 0061 SX = SX + (RM**2+1.)*A(M)**2
ISN 0062 706 SY = SY + A(M)**2
ISN 0063 IF(NV.LE.2) GO TO 712
ISN 0064 NVP = NV-2
ISN 0065 DO 708 M = 1,NVP
ISN 0066 RM = M
ISN 0067 SX = SX - (RM+1.):**2*A(M)*A(M+2)
ISN 0068 708 SY = SY - A(M)*A(M+2)
ISN 0069 712 CONTINUE
ISN 0070 AB2RXX = 12.*PI2*(.75*SX + NU*AB2*SY)
ISN 0071 RYB = 12.*PI2*(AB2*SY + .75*NU*SX)
ISN 0072 PHIPXX = 0.
ISN 0073 PHIPYY = 0.
ISN 0074 DO 702 M = 1,NV
ISN 0075 DO 702 N = 1,NV
ISN 0076 X = B1(M,N)*CS(M-N,XA) + B2(M,N)*CS(M-N-2,XA)
ISN 0077 1 + B3(M,N)*CS(M-N+2,XA) + B4(M,N)*CS(M+N,XA)
ISN 0078 2 + B5(M,N)*CS(M+N-2,XA) + B6(M,N)*CS(M+N+2,XA)
ISN 0079 YMN = -16.*PI2*CS(4,YB)*X
ISN 0080 X = B7(M,N)*CS(M-N,XA) + B8(M,N)*CS(M-N-2,XA)
ISN 0081 1 + B9(M,N)*CS(M-N+2,XA) + B10(M,N)*CS(M+N,XA)
ISN 0082 2 + B11(M,N)*CS(M+N-2,XA) + B12(M,N)*CS(M+N+2,XA)
ISN 0083 YMN = YMN - 4.*PI2*CS(2,YB)*X
ISN 0084 RM = M
RN = N
X = (RM-RN)**2*B1(M,N)*CS(M-N,XA) + (RM-RN-2.):**2*B2(M,N)*
1 CS(M-N-2,XA) + (RM-RN+2.):**2*B3(M,N)*CS(M-N+2,XA)
2 + (RM+RN)**2*B4(M,N)*CS(M+N,XA) + (RM+RN-2.):**2*B5(M,N)
3 *CS(M+N-2,XA) + (RM+RN+2.):**2*B6(M,N)*CS(M+N+2,XA)
ISN 0085 XMN = -PI2*CS(4,YB)*X
ISN 0086 X = (RM-RN)**2*B7(M,N)*CS(M-N,XA) + (RM-RN-2.):**2*B8(M,N)*
1 CS(M-N-2,XA) + (RM-RN+2.):**2*B9(M,N)*CS(M-N+2,XA)
2 + (RM+RN)**2*B10(M,N)*CS(M+N,XA) + (RM+RN-2.):**2*B11(M,N)
3 *CS(M+N-2,XA) + (RM+RN+2.):**2*B12(M,N)*CS(M+N+2,XA)
ISN 0087 XMN = XMN - PI2*CS(2,YB)*X
ISN 0088 X = (RM-RN)**2*B13(M,N)*CS(M-N,XA) + (RM-RN-2.):**2*B14(M,N)*
1 CS(M-N-2,XA) + (RM-RN+2.):**2*B15(M,N)*CS(M-N+2,XA)
2 + (RM+RN)**2*B16(M,N)*CS(M+N,XA) + (RM+RN-2.):**2*B17(M,N)
3 *CS(M+N-2,XA) + (RM+RN+2.):**2*B18(M,N)*CS(M+N+2,XA)

```

ISN 0089		XMN = XMN - PI2*X
ISN 0090		PHIPXX = PHIPXX + XMN*A(M)*A(N)
ISN 0091	702	PHIPYY = PHIPYY + YMN*A(M)*A(N)
ISN 0092		PHIPXX = 12.*(1.-NU**2)*AB2*PHIPXX
ISN 0093		PHIPYY = 12.*(1.-NU**2)*AB2*PHIPYY
ISN 0094		SIGMAX = AB2RXB + AB2*PHIPYY
ISN 0095		SIGMAY = RYB + PHIPXX
ISN 0096		SIGMAX = SIGMAX/12.
ISN 0097		SIGMAY = SIGMAY/12.
	C	PRINT IN-PLANE STRESSES AT POINT(XA,YB)
ISN 0098		WRITE (6,701) SIGMAX, SIGMAY
ISN 0099		XA = XA + 1./16.
ISN 0100	710	CONTINUE
ISN 0101		RETURN
ISN 0102		END

COMPILER OPTIONS - NAME= MAIN,OPT=02,LINECNT=58,SIZE=0000K,
SOURCE,EBCDIC,NOLIST,NODECK,LOAD,MAP,NOEDIT,ID,NOXREF

```
ISN 0002      FUNCTION B13(M,N)
ISN 0003      B13 = 0.
ISN 0004      IF(M-N .NE. 0) B13 = -FLOAT(2*M)/FLOAT((M-N)**3)
ISN 0006      RETURN
ISN 0007      END
```

COMPILER OPTIONS - NAME= MAIN,OPT=02,LINECNT=58,SIZE=0000K,
SOURCE,EBCDIC,NOLIST,NODECK,LOAD,MAP,NOEDIT,ID,NOXREF

```
ISN 0002      FUNCTION B14(M,N)
ISN 0003      B14 = 0.
ISN 0004      IF(M-N-2 .NE. 0) B14 = FLOAT (M-1)/FLOAT ((M-N-2)**3)
ISN 0006      RETURN
ISN 0007      END
```

COMPILER OPTIONS - NAME= MAIN,OPT=02,LINECNT=58,SIZE=0000K,
SOURCE,83CDIC,NOLIST,NODECK,LOAD,MAP,NOEDIT,ID,NOXREF

```
ISN 0002      FUNCTION B15 (M,N)
ISN 0003      B15 = 0.
ISN 0004      IF (M-N+2 .NE. 0) B15 = FLOAT (M+1)/FLOAT ((M-N+2)**3)
ISN 0006      RETURN
ISN 0007      END
```

COMPILER OPTIONS - NAME= MAIN,OPT=02,LINECNT=58,SIZE=0000K,
SOURCE,EBCDIC,NOLIST,NODECK,LOAD,MAP,NOEDIT,ID,NOXREF

```
ISN 0002      FUNCTION B16(M,N)
ISN 0003      B16 = 0.
ISN 0004      IF(M+N .NE. 0) B16 = FLOAT(2*M)/FLOAT((M+N)**3)
ISN 0006      RETURN
ISN 0007      END
```

COMPILER OPTIONS - NAME= MAIN,OPT=02,LINECNT=58,SIZE=0000K,
SOURCE,ZBCDIC,NOLIST,NODECK,LOAD,MAP,NOEDIT,ID,NOXREF

```
ISN 0002      FUNCTION B17 (M,N)
ISN 0003      B17 = 0.
ISN 0004      IF (M+N-2 .NE. 0) B17 = -FLOAT(M-1)/FLOAT((M+N-2)**3)
ISN 0006      RETURN
ISN 0007      END
```

COMPILER OPTIONS - NAME= MAIN,OPT=02,LINECNT=58,SIZE=0000K,
SOURCE,EBCDIC,NOLIST,NODECK,LOAD,MAP,NOEDIT,ID,NOIRBF

```
ISN 0002      FUNCTION E18(M,N)
ISN 0003      B18 = 0.
ISN 0004      IF (M+N+2 .NE. 0) B18 = -FLOAT(M+1)/FLOAT((M+N+2)**3)
ISN 0006      RETURN
ISN 0007      END
```